

13615

NATIONAL LIBRARY  
OTTAWA



BIBLIOTHÈQUE NATIONALE  
OTTAWA

NAME OF AUTHOR. *REBECCA ARRIETA VERMEER*  
 TITLE OF THESIS. *MECHANISM OF ALCOHOL FORMATION*  
*IN LIQUID n-PROPYL*  
*ETHER*  
 UNIVERSITY. *UNIVERSITY of ALBERTA*  
 DEGREE FOR WHICH THESIS WAS PRESENTED. *M.Sc.*  
 YEAR THIS DEGREE GRANTED. *1972*

Permission is hereby granted to THE NATIONAL LIBRARY  
 OF CANADA to microfilm this thesis and to lend or sell copies  
 of the film.

The author reserves other publication rights, and  
 neither the thesis nor extensive extracts from it may be  
 printed or otherwise reproduced without the author's  
 written permission.

(Signed) *Rebecca Vermeer*

PERMANENT ADDRESS:

*3 PINE ST*  
*SHERWOOD PARK*  
*ALBERTA*

DATED *June 28* 19 *72*

NL-91 (10-68)

THE UNIVERSITY OF ALBERTA

MECHANISM OF ALCOHOL FORMATION IN LIQUID  
n-PROPYL ETHER RADIOLYSIS : ELECTRON REACTIONS

by



REBECCA ARRIETA VERMEER

A THESIS

SUBMITTED TO THE FACULTY OF GRADUATE STUDIES AND RESEARCH  
IN PARTIAL FULFILMENT OF THE REQUIREMENTS FOR THE DEGREE

OF

MASTER OF SCIENCE

DEPARTMENT OF CHEMISTRY

EDMONTON, ALBERTA


FALL 1972

THE UNIVERSITY OF ALBERTA  
FACULTY OF GRADUATE STUDIES AND RESEARCH

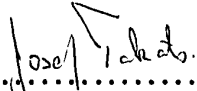
The undersigned certify that they have read,  
and recommend to the Faculty of Graduate Studies  
and Research for acceptance, a thesis entitled

"MECHANISM OF ALCOHOL FORMATION IN LIQUID n-PROPYL  
ETHER RADIOLYSIS : ELECTRON REACTIONS"

submitted by REBECCA ARRIETA VERMEER in partial  
fulfilment of the requirements for the degree of  
Master of Science.

  
.....  
Supervisor

  
.....

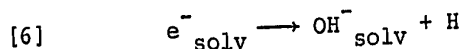
  
.....

  
.....

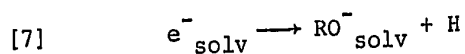
.....  
Date June 26/72

A B S T R A C T

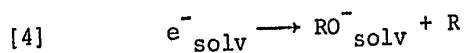
The study of the mechanism of alcohol formation in the  $\gamma$ -radiolysis of liquid n-propyl ether provides information as to the nature of solvated electron reactions in ethers. In water, the solvated electrons can decompose by reaction



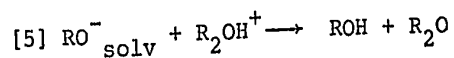
Similarly, in alcohols



There has been no evidence that the solvated electrons in ether can decompose in an analogous way.

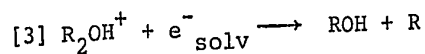


Reaction [4] would probably be followed by



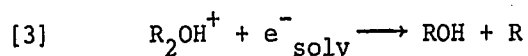
with the formation of alcohol.

A mechanism that has been proposed for the formation of alcohol in diethyl ether (2) is



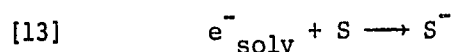
To determine whether alcohol is formed by reaction [3] or [5], various scavengers were added to n-propyl ether. The additions of sulfur hexafluoride and n-propylamine decreased the propanol yield suggesting that  $e^-_{\text{solv}}$  and  $\text{R}_2\text{OH}^+$

are the precursors of alcohol. The effects of both n-propylamine and hydrogen chloride on the yield of alcohol ruled out reactions [4] and [5] and supported the reaction



as the source of propanol. Reaction [3] occurs in the spurs.

The scavenging studies provided evidence for the participation of solvated electrons in a spur reaction during radiolysis of n-propyl ether. Direct observation of solvated electrons during pulse radiolysis confirmed its presence in a radiolysis system. The pulse radiolysis technique allows the observation of solvated electrons in the bulk medium by means of its absorption spectrum and half-life in a given reaction. Absorption spectra of solvated electrons from 600-1600 nm were obtained at temperatures 0°, -73° and -133°C. At all three temperatures, the absorption maxima lay above 1600 nm, being the limit of the detection equipment. The absorption maximum shifted to lower wavelengths with decreasing temperature as indicated by the change in the shape of the spectrum. The decay of solvated electrons in the bulk medium is believed to be a reaction with impurity, S.



The activation energy for reaction [13] is 3 kcal/mole. The same activation energy was obtained for the reaction of solvated electrons with sulfur hexafluoride.

ACKNOWLEDGEMENTS

I am most grateful to Professor G. R. Freeman for his guidance during the study.

I appreciate the helpful discussions with Dr. K. N. Jha and members of the Radiation Chemistry group.

The assistance of R. Gardner and F. Bach during pulse radiolysis experiments and the typing of the thesis by M. Waters are gratefully acknowledged.

I thank my husband, Kees, for his encouragement.

<u>T A B L E O F C O N T E N T S</u>		<u>Page</u>
ABSTRACT . . . . .		iii
ACKNOWLEDGEMENTS . . . . .		v
TABLE OF CONTENTS . . . . .		vi
LIST OF TABLES . . . . .		ix
LIST OF FIGURES . . . . .		x
I	INTRODUCTION	
	A. General Review . . . . .	1
	B. Solvated Electrons . . . . .	3
	1. Production of Solvated Electrons . . . . .	4
	2. Evidence for Solvated Electrons . . . . .	5
	3. Reactions of Solvated Electrons . . . . .	9
	4. Structure of Solvated Electrons . . . . .	12
II	$\gamma$ -RADIOLYSIS OF n-PROPYL ETHER	
	A. Experimental. . . . .	14
	Part I. Materials . . . . .	14
	Part II. Procedures and Techniques . . . . .	17
	1. Sample Preparation. . . . .	17
	2. Sample Irradiation . . . . .	18
	3. Product Analysis . . . . .	18
	4. Determination of Sulfur Hexafluoride Solubility. . . . .	20
	5. Determination of the Density of n-Propyl Ether . . . . .	21

	B. Results . . . . .	27
	Part I. n-Propyl Ether . . . . .	27
	Part II. Ether-Sulfur Hexafluoride Solutions . .	27
	Part III. Ether-Hydrogen Chloride Solutions . .	35
	Part IV. Ether-Sulfuric Acid Solutions . . . . .	35
	Part V. Ether-n-Propylamine Solutions . . . . .	36
	Part VI. Ether-Propylene Solutions . . . . .	36
III	PULSE RADIOLYSIS OF n-PROPYL ETHER	
	A. Experimental. . . . .	43
	Part I. The Pulse Radiolysis Experiment . . . .	43
	Part II. Components of the Pulse Radiolysis Apparatus . . . . .	45
	B. Results . . . . .	53
	Part I. Absorption Spectra of Solvated Electrons	53
	Part II. Order of Reaction, Half-life and Rate Constant . . . . .	53
	Part III. Activation Energy . . . . .	61
IV	DISCUSSION. . . . .	63
	A. Mechanism . . . . .	64
	B. Kinetics . . . . .	68
	Part I. Homogeneous Kinetics of $e^-_{\text{solv}}$ (free ion) Reactions . . . . .	71
	Part II. Application of Non-homogeneous Kinetic Model . . . . .	75
	C. Solvated Electron Optical Absorption Spectrum . . . . .	79



V	CONCLUSION . . . . .	80
	REFERENCES . . . . .	81
	APPENDIX . . . . .	85



LIST OF TABLES

<u>Table</u>		<u>Page</u>
I	Determination of Charge on $e^-_{\text{solv}}$	8
II	Ostwald Absorption Coefficient ( $\alpha$ ) of Sulfur Hexafluoride in n-Propyl Ether	22
III	Volume-Temperature Data on n-Propyl Ether	22
IV	n-Propanol Yield as a Function of Sulfur Hexafluoride Concentration and Time Irradiated Sample Stood Before Analysis	28
V	n-Propanol Yield as a Function of Time Sample Stood After Irradiation	30
VI	Product Yields as a Function of Sulfur Hexafluoride Concentration	33
VII	Product Yields as a Function of Hydrogen Chloride Concentration	37
VIII	n-Propanol Yield as a Function of n-Propylamine Concentration	39
IX	n-Propanol Yield as a Function of Propylene Concentration	41
X	Order of Reaction, Half-life and Rate Constants of Solvated Electron Reactions	54
XI	Electron and Positive Ion Mobilities at $\sim 23^\circ\text{C}$	78

LIST OF FIGURES

<u>Figure</u>		<u>Page</u>
1	Effect of Ionic Strength on Relative Rate Constants of $e^-_{\text{solv}}$ Reactions	7
2A	Sample Preparation Manifold	23
2B	Main Vacuum Line	24
3	Vacuum System for Solubility Measurement	25
4	n-Propanol Yield as a Function of Sulfur Hexafluoride Concentration and Time Irradiated Sample Stood Before Analysis	29
5	Dependence of n-Propanol Yield on Time Irradiated Sample Stood Before Analysis	31
6	n-Propanol Yield as a Function of Sulfur Hexafluoride Concentration	34
7	n-Propanol Yield as a Function of Hydrogen Chloride Concentration	38
8	n-Propanol Yield as a Function of n-Propylamine Concentration	40
9	n-Propanol Yield as a Function of Propylene Concentration	42
10	Pulse Radiolysis Equipment	44
11	Time Delay for Absorption Signal and Electron Signal	46
12	Secondary Emission Monitor (SEM)	52
13	Absorption Spectra of Solvated Electrons	55

<u>Figure</u>		<u>Page</u>
14A	Representative Absorption Signals	56
15A-15C	Plots of Reaction Order	58,59,60
16	Arrhenius Plot for Rate Constants of $e^-_{\text{solv}}$ Reactions	62
17	Calculated Spectra of Lifetimes of Solvated Electrons	74

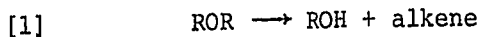
---

## I. INTRODUCTION

### A. General Review

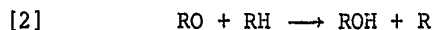
A survey of the liquid phase radiolysis of some aliphatic ethers with helium ions was made by Newton (1). Alcohols were among the major products of radiolysis. Product yields were reported as G values, the number of molecules formed per 100 ev of energy absorbed. In the case of di-n-propyl ether, Newton (1) found that the major products were hydrogen ( $G = 2.74$ ), "polymers" ( $G \sim 1.6$ ), carbonyl compounds ( $G = 1.36$ ), alcohols, reported as hydroxyl compounds ( $G = 1.30$ ), propylene ( $G = 0.49$ ) and propane ( $G = 0.43$ ). From the yields of hydrocarbons, it was found that the rupture of C-O bonds was more extensive than that of C-C bonds. Ng (2) obtained from radiolysis studies of diethyl ether the relative probabilities of cleavage of the various bonds. They are C-O ( $G = 1.6$ ) >> C-H ( $G = 0.34$ ) > C-C ( $G = 0.28$ ).

The formation of alcohol in ether was suggested to result from a C-O bond cleavage involving a molecular rearrangement with hydrogen atoms on the  $\beta$ -carbon atom (1).

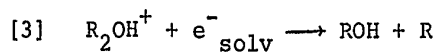


Scavenging studies (2) on diethyl ether gave further information on the reaction mechanism of alcohol formation. Ng found that only about half of the ethanol yield was

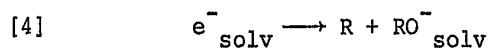
scavengeable by 1,3-pentadiene (2). He suggested reaction [1] as the mechanism for the unscavengeable yield. Being a conjugated di-olefin, 1,3-pentadiene could scavenge either free radicals (3) or electrons (4). The mechanism proposed for the scavengeable yield of alcohol is (2)



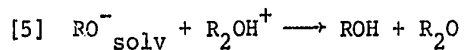
where RH is a free radical or molecule, or a neutralization reaction



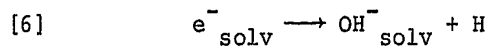
An alternative reaction of solvated electrons which could lead to alcohol formation is the decomposition reaction



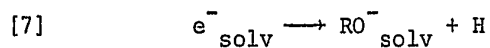
followed by



Reaction [4] is analogous to the decomposition reaction of solvated electrons which occurs in water



and in alcohols



The first order half-life for the decomposition reaction in water is 0.8 milliseconds, while in alcohols it is of the order of microseconds (5).

There has been no evidence that reaction [4] occurs in ether as in water or alcohols. The study of the mechanism of n-propanol formation during  $\gamma$ -radiolysis of liquid n-propyl ether will provide evidence as to whether the solvated electron reaction [4] occurs in ether. The mechanism of alcohol formation was investigated by means of scavenging studies. The participation of solvated electrons in reactions during radiolysis was studied by pulse radiolysis experiment.

In the remainder of this Chapter, the nature of solvated electrons is discussed.

#### B. Solvated Electrons

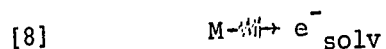
A solvated electron is an extra-molecular electron localized in a cavity of the medium in which the dielectric has relaxed around it (6). The solvated electron is in thermal equilibrium with the medium. Solvated electrons occur in many liquids such as water, ammonia, amines, alcohols and ethers. They have low mobilities which are  $< 1 \text{ cm}^2/\text{V sec}$ . They are characterized by optical absorption, paramagnetism and electrical conductivity. The absorption bands are broad with maxima lying in the visible or near infrared regions. These properties characterize the

solvated electrons in various media subjected to high energy radiation.

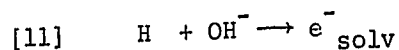
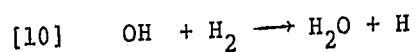
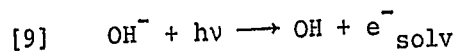
The existence of solvated electrons in radiation chemistry was not confirmed until the early sixties. It continued to be mistaken for the hydrogen atom until it was demonstrated that the major reducing species in irradiated water has a unit negative charge (7) and was responsible for the transient absorption spectrum in the pulse radiolysis of aqueous solutions (8,9).

#### 1. Production of Solvated Electrons

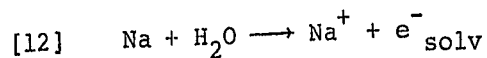
Solvated electrons are generated directly by radiolysis



In the flash photolysis of hydrogen saturated 0.001 N sodium hydroxide solution, solvated electrons are formed by the following mechanism (10):



The reaction of an alkali metal generates solvated electrons (11).





## 2. Evidence for Solvated Electrons

The determination of the charge of the major reducing species in irradiated water and the discovery of a transient absorption spectrum bearing the properties of a solvated electron presented important evidence for the existence of solvated electrons.

The magnitude and sign of the charge on the reducing species were determined using the Bronsted-Bjerrum theory of ionic reactions (12). The theory states that the rate constant ( $k$ ) at ionic strength ( $\mu$ ) will increase, decrease or remain constant depending respectively, on whether the charges of the reactants are of the same sign, opposite signs or one is zero. This is given for aqueous solutions by the equation

$$[i] \quad \log_{10} \frac{k}{k_0} = 1.02 (Z_{\text{red}})(Z_s) \frac{\mu^{\frac{1}{2}}}{1 + \alpha(\mu)^{\frac{1}{2}}}$$

where  $k_0$  is the rate constant at zero ionic strength,  $Z_{\text{red}}$  and  $Z_s$  are the charges on the reducing species and solute respectively, and  $\alpha$  is a parameter whose value is close to unity and taken as such. If  $Z_s$  is known, a determination of the dependence of  $k$  on  $\mu$  permits an evaluation of the magnitude and sign of  $Z_{\text{red}}$ .

Since absolute rate constants could not be determined in 1962 for lack of suitable techniques, Czapski and Schwartz (7) compared the effect of  $\mu$  on relative rate constants.

They compared the rates of the reaction of the reducing species with  $\text{NO}_2^-$ ,  $\text{H}^+$  and  $\text{O}_2$  to the rate of the reaction with  $\text{H}_2\text{O}_2$  as a function of ionic strength. The results are shown in Figure 1 and Table I. In Figure 1, K represents the ratio  $k_{(\text{red} + \text{s})}/k_{(\text{red} + \text{H}_2\text{O}_2)}$  at ionic strength  $\mu$  and  $K_0$  is that ratio when  $\mu = 0$ . The slopes of the lines drawn show that Z for the reducing species was -1. The same conclusion was reached by Collinson *et.al.* (13). It was concluded that the reducing species was  $e^-_{\text{solv}}$ .

The effect of ionic strength on the rate constant ratios has also been studied in the  $\gamma$ -radiolysis of methanol (14). The results indicate that the reducing species in methanol has a unit negative charge, i.e. that it is the solvated electron.

The emergence of pulse radiolysis techniques made possible the observation of transient absorptions in an irradiated liquid and led to the establishment of the identity of the major reducing species. In water (8,9) an absorption band was obtained with a maximum at  $7200 \text{ \AA}$ . This was assigned to the solvated electron. The evidence for the assignment of this absorption band to  $e^-_{\text{solv}}$  is:

- (a) Electron scavengers such as  $\text{H}^+$ ,  $\text{O}_2$ ,  $\text{H}_2\text{O}_2$ ,  $\text{N}_2\text{O}$  and  $\text{CO}_2$  accelerated the decay of  $e^-_{\text{solv}}$  and at sufficiently

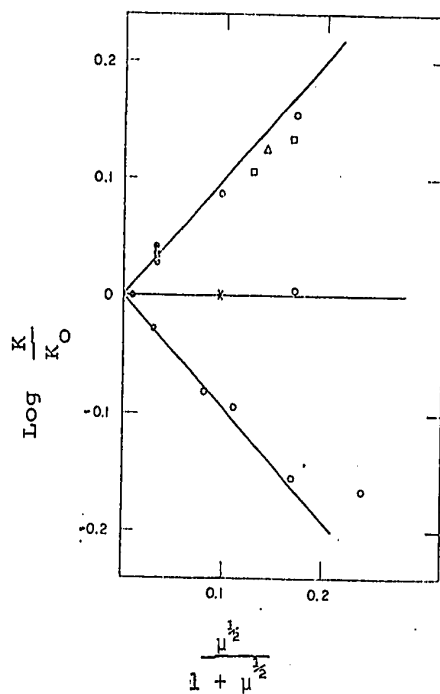


**FIGURE 1** Effect of ionic strength on relative rate constants for reactions of  $e^-_{\text{solv}}$  with various solutes (7). Upper curve,  $\text{NO}_2^-$  relative to  $\text{H}_2\text{O}_2$ ; middle curve,  $\text{O}_2$  relative to  $\text{H}_2\text{O}_2$ ; lower curve,  $\text{H}^+$  relative to  $\text{H}_2\text{O}_2$ . The ionic strength was varied with  $\text{LiClO}_4$ ,  $\circ$ ;  $\text{KClO}_4$ ,  $\square$ ;  $\text{NaClO}_4$ ,  $\Delta$ ; and  $\text{MgSO}_4$ ,  $\times$ . The closed circles represent no added salt other than the reactants.

TABLE IDetermination of Charge on  $e^-_{\text{solv}}$ 

S	Solute Reference	$z_s$	Slope* ( $z_s \cdot z_{\text{red}}$ )	$z_{e^-_{\text{solv}}}$
$\text{NO}_2^-$	$\text{H}_2\text{O}_2$	-1	+1	-1
$\text{O}_2$	$\text{H}_2\text{O}_2$	0	0	
$\text{H}^+$	$\text{H}_2\text{O}_2$	+1	-1	-1

\*  
From Figure 1

9.

high concentrations, suppressed or even eliminated the absorption (8).

- (b) The absorption spectrum of the ammoniated electron was similarly affected by electron scavengers (8).

Other studies on this absorption band gave further evidence that it is due to solvated electron.

- (c) Kinetic ion-strength effects have shown that the band was due to a species having a unit negative charge (15).

- (d) Rate constants calculated from the decay of this absorption in the presence of scavengers gave rate constant ratios which agree with those obtained by competitive studies with the same scavengers in steady radiolysis (16).

Subsequently, solvated electron spectra have been obtained in other compounds such as alcohols (17), amines (18,19) and ethers (19,20,21).

### 3. Reactions of Solvated Electrons

The pulse radiolysis technique made possible the determination of absolute rate constants for a variety of reactions of solvated electrons. The rates of these reactions range from  $16 \text{ M}^{-1} \text{ sec}^{-1}$  in water, to  $10^{11} \text{ M}^{-1}$

$\text{sec}^{-1}$  in other cases, many of which are diffusion controlled. In all direct kinetic measurements, the solvated electron is generated in concentrations of  $10^{-8}$  -  $10^{-6}$  M while the reactants are present in much greater concentration. Under these conditions, pseudo-first-order decay of the solvated electron is observed. The rate constants for such reactions are obtained from the observed half-life of the solvated electron.

Reactions of solvated electrons are electron attachment in nature. They involve the transfer of the electron from its site in the solvent into a vacancy in the accepting solute. The reactivity of organic solutes toward solvated electrons differs considerably. The availability of a vacant orbital governs the reactivity of a solute. The following is a grouping of compounds and their reactivity towards solvated electron in water.

- (a) Organic compounds composed of H, C, O and N atoms only and containing no  $\pi$ -bonds are nonreactive (22a).
- (b) The reactivity of alkenes is a function of the group adjacent to the double bond. Reactivity of a non-activated C=C double bond is low ( $k \sim 10^6 \text{ M}^{-1} \text{ sec}^{-1}$ ). The presence of electron withdrawing groups and conjugating C=C double bond greatly enhances the react-

ivity of the C=C bond, increasing the rate constants to  $\sim 10^9 - 10^{10} \text{ M}^{-1} \text{ sec}^{-1}$  (22b).

- (c) Aldehydes, ketones and carboxylic acids have high reactivity. The reactivity of the carbonyl group C=O is decreased by electron withdrawing groups. This is attributed to the decrease in the C=O bond length. As the C=O bond shortens, the electron density in the  $\pi$  orbital increases, resulting in a decreased tendency of the bond to accommodate another electron (22c).
- (d) Alkyl halides are particularly reactive toward solvated electrons with reactivities in the order  $\text{F} \ll \text{Cl} < \text{Br} < \text{I}$  (23). The probability of the electron being attached to a halogen atom increases with the number of orbitals in the atom. The electron-withdrawing capacity of the alkyl groups, expressed in terms of the Taft  $\sigma^*$  function, affects the reactivity of the halide.
- (e) The reactivities of aromatic compounds range over four orders of magnitude, from  $k = 4 \times 10^6$  for phenol to  $k = 3 \times 10^{10} \text{ M}^{-1} \text{ sec}^{-1}$  for nitrobenzene. The reactivity is correlated with the substituents on the benzene ring by means of the Hammett  $\sigma$  function. Electron withdrawing substituents greatly enhance the reactivity of the benzene ring. The reactions of

solvated electrons with aromatic compounds involve an interaction of the electron with the  $\pi$ -orbitals of the ring. Exceptions are the bromo and iodo aromatic derivatives where the electron may interact through the ring or through the halogen atom (22d).

#### 4. Structure of Solvated Electrons

A solvated electron can be qualitatively described as an extra electron trapped in a pre-formed cavity of a liquid. The trapping of the extra electron in a cavity results when its total energy (kinetic and potential energy arising from coulombic repulsion) is less than the potential energy barrier caused by coulombic attraction between the electron and the positive dipoles of a partially relaxed dielectric. The trapped electron transforms into the solvated state when complete dielectric relaxation occurs (24a).

The electron-in-a-cavity model is supported by some experimental evidence and theoretical investigations. In water and in alcohols the energy of the absorption maximum  $E_{\lambda_{\max}}$  was found to decrease with increasing temperature (25,26) and to increase with increasing pressure (27,28). The displacement of the absorption maximum to higher energies with increasing pressure has been ascribed to the compression of the cavity. The displacement toward lower energies with increasing temperature is due to thermal expansion of the cavity (29).



Theoretical models have been devised to predict the energy of the absorption maximum based on the approximation of the liquid as a continuous dielectric medium with the electron trapped in a cavity of the liquid. A theoretical treatment that has met considerable success in predicting some properties of solvated electron in liquid ammonia is Jortner's self consistent field (SCF) approximation (30,31). The energy of the absorption maximum,  $E_{\lambda_{\max}}$ , is interpreted as the energy of transition from a ground to an excited state. The energy of the electron arises from the contributions of orientational and electronic polarization energies. With the use of hydrogenic wave functions for a 1s ground state and a 2p excited state, a value for the energy of 1s  $\rightarrow$  2p transition of 0.81 eV was obtained when a cavity radius of 3.2 Å was assumed. This compares well with the experimental value of  $E_{\lambda_{\max}} = 0.80$  eV (32)..

A similar treatment was applied to the solvated electron in water (31). A reasonable agreement was obtained between the 1s  $\rightarrow$  2p transition energy of 1.8 eV and the experimental value of  $E_{\lambda_{\max}} = 1.72$  eV (33) when a cavity radius of 1.5 Å was assumed.

## II    $\gamma$ -RADIOLYSIS OF n-PROPYL ETHER

The mechanism of alcohol formation in the  $\gamma$ -radiolysis of n-propyl ether can be elucidated by means of scavenging studies. Scavenging is a term applied to the action of an added solute (scavenger) which reacts preferentially with one of the reactants of the radiolysis reaction. The reaction by which alcohol is formed was investigated with the following scavengers: sulfur hexafluoride, an electron scavenger; n-propylamine, a positive-ion scavenger; acid, an electron scavenger; and propylene, a free radical scavenger. The effects of these scavengers on the radiolysis yield of propanol provide evidence as to the identities of the precursors of propanol.

### A.    Experimental

#### Part I.    Materials

1.    n-Propyl ether: n-propyl ether was obtained from Eastman Organic Chemicals and from Aldrich Chemical Company (Gold Label quality). The ether was purified as follows: The peroxide content of the ether was qualitatively determined with a glacial acetic acid-potassium iodide solution. High peroxide concentration around  $10^{-3}$  M was indicated by a dark brown coloration. It was removed by passing the ether through a 14" x 3/4" neutral Woelm Alumina column to prevent peroxide explosion during distil-

lation. Most of the propionaldehyde was removed by adding 1.5 g of 2,4-dinitrophenylhydrazine and 2 ml of concentrated sulfuric acid to 700 ml of ether and refluxing the solution for 20 hours. Most of the propanol and other impurities were removed by fractional distillation through a 24" Vigreux column packed with glass beads. The purity of the distillate was checked by gas chromatography. About 300 ml of the prime distillate was passed through two 14" x 3/4" neutral Woelm Alumina columns to remove traces of remaining impurities. No propionaldehyde, propanol or 1,1-dipropoxypropane impurity were detected on gas chromatographic analysis of the purified ether at a sensitivity of  $1 \times 10^{-4}$  M. The purified ether was degassed and stored under vacuum over a sodium mirror.

2. Sulfur Hexafluoride: Sulfur hexafluoride from Matheson of Canada Ltd. was purified by trap-to-trap sublimation in a vacuum apparatus and stored in a Pyrex reservoir.
3. Hydrogen Chloride: Anhydrous hydrogen chloride from Matheson of Canada Ltd. was purified by passing over copper foil to remove chlorine followed by trap-to-trap sublimation under vacuum. It was stored in a Pyrex reservoir.
4. Propylene: Propylene from Matheson of Canada Ltd.

was purified by trap-to-trap distillation under vacuum and stored in a Pyrex reservoir.

5. n-Propylamine: n-Propylamine from Eastman Organic Chemicals was purified by fractional distillation. A distillate portion was further purified by repeated freeze-pump-thaw cycles under vacuum. It was stored in a Pyrex reservoir fitted with a Hoke valve (stainless steel needle and teflon seat).

6. Sulfuric Acid: Reagent grade acid from C.I.L. was used as received.

7. 1-Propanol: Certified grade from Fisher Scientific Company was used as received.

8. Propionaldehyde: Obtained from Eastman Organic Chemicals and used as received.

9. 1,1-Dipropoxypropane: 1,1-Dipropoxypropane was prepared using approximately 10 g anhydrous copper sulfate in 500 ml solution of 25% propionaldehyde in 1-propanol. The solution was shaken, then allowed to stand overnight. Copper sulfate was removed by centrifuge and excess alcohol removed by rotary evaporation. The crude product was purified by fractional distillation under vacuum (about 30 microns pressure) with the pot at room temperature and the receiver cooled to  $-80^{\circ}\text{C}$  (dry ice temperature). The

fraction used for a standard was 96% pure.

Anhydrous copper sulfate was prepared by heating copper sulfate hydrate to 180° - 200°C under vacuum until colorless.

## Part II Procedures and Techniques

### 1. Sample Preparation (Fig. 2A, 2B)

Three types of Pyrex sample cells were used: Cell A which was used for a sample with gas additive whose absorption coefficient ( $\alpha$ ) had been determined; Cell B when a liquid additive was added externally; and Cell C when a large volume<sub>(liquid)</sub>/volume<sub>(gas)</sub> ratio was needed. The volumes of the cells were approximately 6 ml, 6 ml and 2 ml respectively. The cells were cleaned with concentrated sulfuric acid-potassium permanganate solution, rinsed with water and then rinsed with dilute nitric acid-hydrogen peroxide solution. The cells were rinsed repeatedly with triply distilled water and dried overnight in an oven at 150°C. The cells were evacuated overnight before filling them.

Samples were prepared by vacuum distilling the ether from the reservoir into the measuring tube cooled to 0°C with an ice-water bath. Volumes of 1.8 and 2 ml were used. The measured volume of ether was distilled into the trap at liquid nitrogen temperature (-196°C), degassed and distilled into the sample cell. Additives such as sulfur hexa-

fluoride, hydrogen chloride, propylene and n-propylamine were measured in the vapor phase (volume, pressure and temperature) and were condensed into the frozen samples. The cell was sealed off with the sample frozen at  $-196^{\circ}\text{C}$ . For the sulfuric acid solutions, a known volume of acid was delivered quickly into the cell from a syringe with a stainless steel needle. The acid was frozen with liquid nitrogen then degassed by successive pump-thaw-freeze-pump cycles. Degassed ether of known volume was distilled into the cell and the cell sealed off.

## 2. Sample Irradiation

The irradiation source was a Gammacell-220 (Atomic Energy of Canada Ltd.) containing 6000 Curies of  $^{60}\text{Co}$ . All samples were irradiated at one position in the sample holder at  $23 \pm 2^{\circ}\text{C}$ . Dosimetry was carried out with a Fricke dosimeter. The Fricke solution was 1 mM in  $\text{Fe}(\text{NH}_4)_2(\text{SO}_4)_2$ , 1 mM in NaCl and 0.8 N in  $\text{H}_2\text{SO}_4$ . Dosimetry calculations were based on the values  $G(\text{Fe}^{+3}) = 15.5$ ,  $\epsilon(\text{Fe}^{+3})$  at  $304 \mu = 2225 \text{ l mole}^{-1} \text{ cm}^{-1}$  at  $25^{\circ}\text{C}$  and a temperature coefficient of  $\epsilon(\text{Fe}^{+3})$  of  $0.7\%/^{\circ}\text{C}$  (34). The dose rate was approximately  $3 \times 10^{19} \text{ eV gm}^{-1} \text{ hr}^{-1}$  in ether and was continuously corrected for the radioactive decay of the  $^{60}\text{Co}$  ( $t_{1/2} = 5.27 \text{ yr}$ ).

## 3. Product Analysis

The products measured in the analyses of irradiated

propyl ether were propanol, propionaldehyde, 1,1-dipropoxypropane, 1-propyl chloride and 2-propyl chloride. The analyses were done with a gas chromatograph consisting of an Aerograph Autoprep 705 with flame ionization detector and a Minneapolis-Honeywell Reg. Co. recorder. Calibrating standards of propanol, propionaldehyde and 1-propyl chloride were used daily. A response ratio of propanol to 1,1-dipropoxypropane was used to calculate the concentration of the latter in the irradiated sample. The percent 2-propyl chloride formed with respect to 1-propyl chloride was used to calculate the 2-propyl chloride concentration in the sample.

A 2  $\mu$ l sample was injected into a column, using a 10  $\mu$ l syringe fitted with a Chaney adapter (constant volume adapter). Four different columns were used depending on the nature of the additive and the product analyzed. A 6' x 1/8" stainless steel column packed with 10% 1,2,3-tris(2-cyanoethoxy)propane (TCEP) on chromosorb W.A.W. was used for propanol and 1,1-dipropoxypropane measurements in all irradiated samples except those with added n-propylamine and hydrogen chloride in high concentrations. Samples containing sulfuric acid were injected through a 1" x 1/4" pre-column packed with potassium hydroxide pellets to remove the acid before analysis. A 2' x 1/8" glass column packed with Porapak Q was used for samples with n-propylamine additive. Alcohol standards and some irradiated

samples were made 0.1 M in amine prior to injection. A 4' x 1/8" stainless steel column packed with Porapak T was used for propanol, 1-propyl chloride and 2-propyl chloride measurements in samples with added hydrogen chloride in high concentrations. Samples analyzed for propionaldehyde were run on a 6' x 1/8" stainless steel column packed with 10% Carbowax 1540 on Porapak P.

Column temperatures were kept at 65 - 100°C for the TCEP column, 85°C for Carbowax 1540, 120°C for Porapak Q and 135°C for Porapak T. Injector temperature was 130°C and the detector temperature was 220°C.

#### 4. Determination of Sulfur Hexafluoride Solubility

The Ostwald absorption coefficient ( $\alpha$ ) of sulfur hexafluoride in propyl ether was measured at -76°, 0° and 25°C using the system shown in Figure 3.  $\alpha = C_{\text{liquid}}/C_{\text{gas}}$  where  $C_{\text{liquid}}$  and  $C_{\text{gas}}$  are the concentrations of sulfur hexafluoride in the liquid and gas phases at a given temperature.

A 10 ml volume of degassed ether was introduced into the bulb from the ether line (Figure 2A). A measured amount of sulfur hexafluoride (volume, pressure and temperature) was condensed into the ether bulb with liquid nitrogen. The solution was stirred with a magnetic stirrer while warming up to the required temperature. For  $\alpha$  determination at 25°C, the solution was allowed to warm



up to room temperature; at 0°C, the solution was warmed to above zero and then cooled with an ice-water bath; and at -76°C, the solution was warmed to near zero and then cooled with an acetone-dry ice bath. The ether volume and a known volume above the liquid were cooled to the required temperature. When equilibrium was reached, the pressure and volume of the gas above the liquid were measured to determine the concentration of undissolved gas. Three runs were made at each temperature over a four-fold range in pressure of sulfur hexafluoride. The volume occupied by the gas above the liquid ether was about 1.5 times the volume of the liquid in all the runs. The values are shown in Table II.

5. Determination of the Density of n-Propyl Ether

The density of propyl ether at -73° and -133°C was needed to determine the molarity of a solution at these temperatures. To obtain these values, a temperature-volume relation was determined for the ether at temperatures 0°, -42°, -87° and -112.5°C using an ice-water bath, liquid nitrogen-chlorobenzene slush, nitrogen-ethylacetate slush and nitrogen-ethanol slush baths, respectively. The calibrated measuring tube in Figure 2A was used in the measurements. The volume-temperature data is shown in Table III. A linear relation was obtained between temperature and volume. The volume at -133°C was obtained by extrapolating

TABLE II

Ostwald Absorption Coefficient ( $\alpha$ ) of  
Sulfur Hexafluoride in n-Propyl Ether

<u>Temperature</u>	<u><math>\alpha</math></u>
25°C	1.70
0°C	2.15
-76°C	2.40

---

TABLE III

Volume-Temperature Data on n-Propyl Ether

<u>Temperature</u>	<u>Volume (cc)</u>
0°C	3.00
-42°C	2.86
-87°C	2.72
-112.5°C	2.64

---

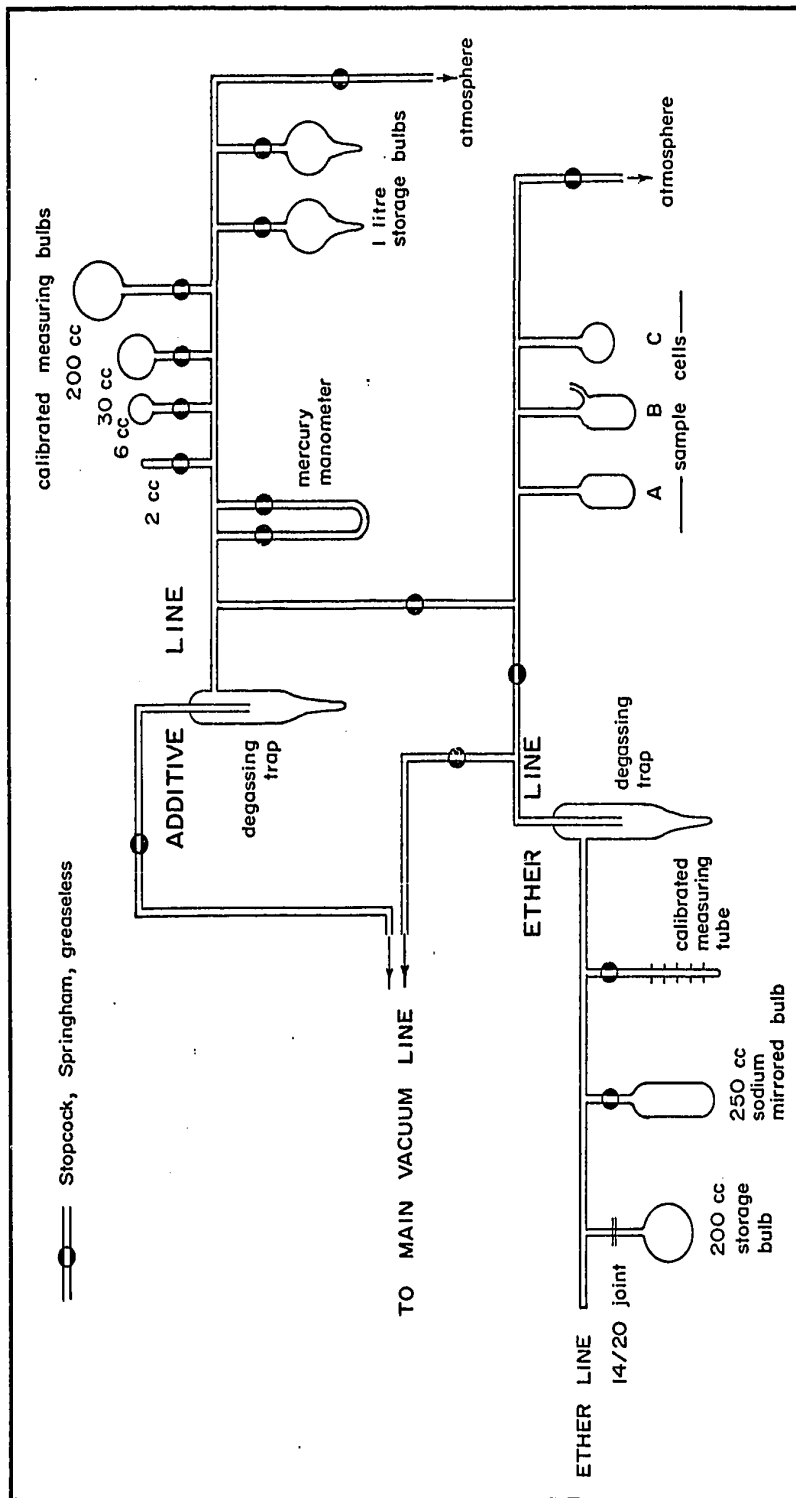


Figure 2A : SAMPLE PREPARATION MANIFOLD

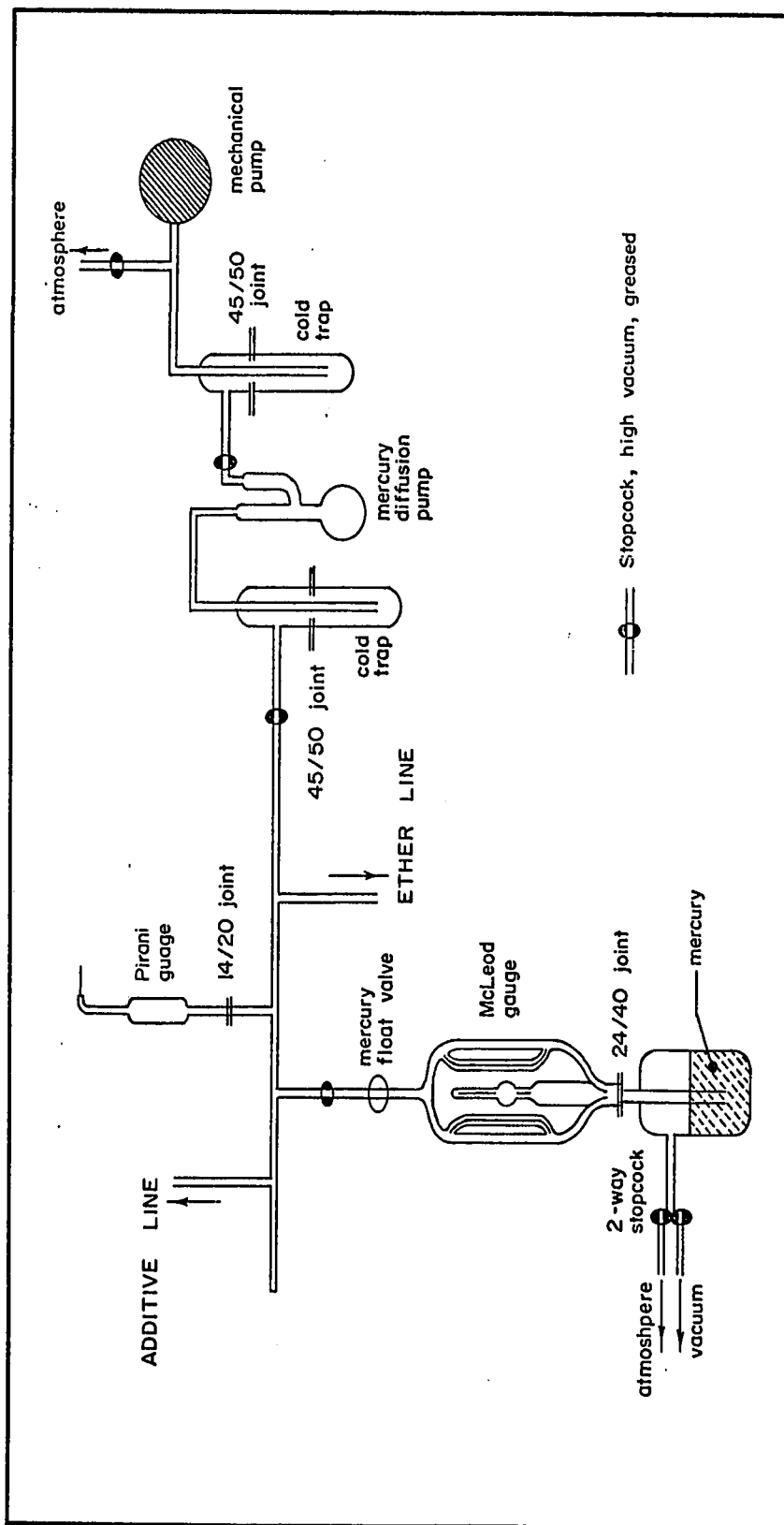


Figure 2B : MAIN VACUUM LINE

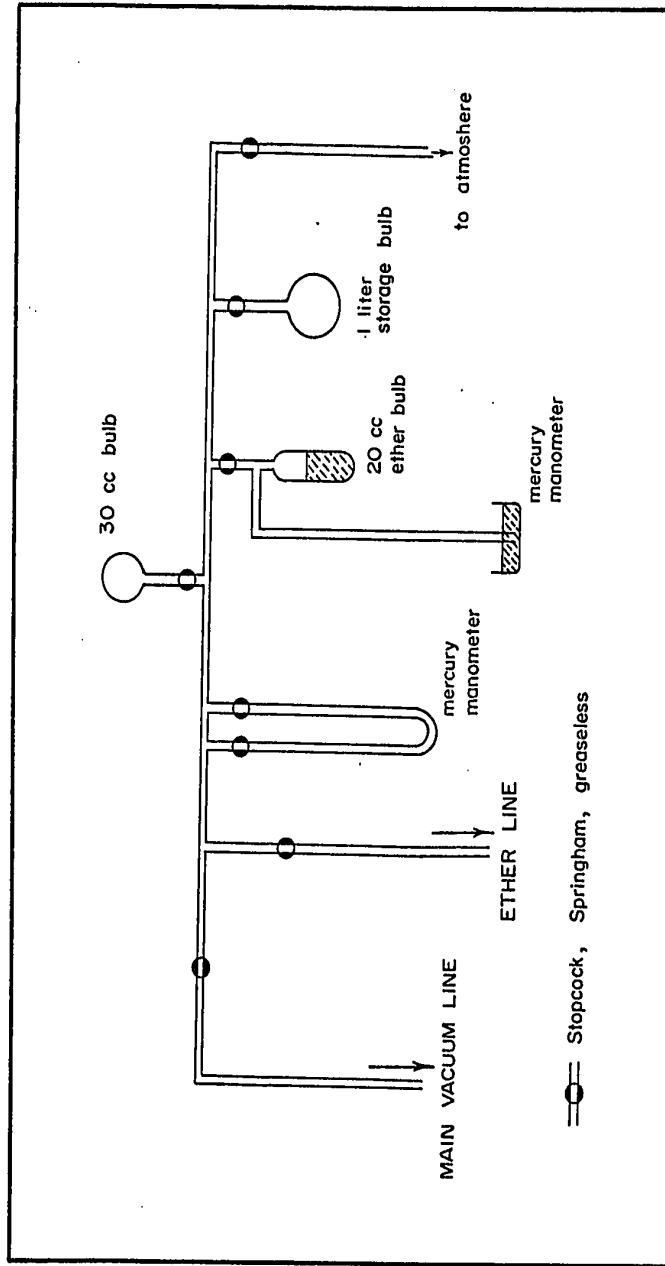


Figure 3 : VACUUM SYSTEM FOR SOLUBILITY MEASUREMENT

the line. Given the density of ether  $D = 0.766$  g/cc at  $0^{\circ}\text{C}$  (35), the densities at  $-73^{\circ}$  and  $-133^{\circ}\text{C}$  are 0.826 and 0.891 g/cc, respectively.

## B Results

### Part I n-Propyl Ether

Radiolysis of n-propyl ether in three different cells gave product yields of  $G = 2.50$  for propanol,  $G = 0.30$  for propionaldehyde and  $G = 0.01$  for 1,1-dipropoxypropane. The propanol yield was independent of the time the irradiated samples stood before analysis.

### Part II Ether-Sulfur Hexafluoride Solutions

1. The yield of propanol as a function of sulfur hexafluoride concentration and approximate time which the irradiated sample stood before analysis is presented in Figure 4 and Table IV. The  $G(1-C_3H_7OH)$  vs  $[SF_6]$  data which appeared to have a bad scattering of points, was found to have a time-dependence when the points were grouped into time ranges which the irradiated samples stood before analysis. The trend shows that the alcohol yield tends to decrease with time and with increasing concentration of sulfur hexafluoride.

2. The above trend of decreasing alcohol yield with time was further investigated in a time study. Samples which were made  $9 \times 10^{-3}$  M ( $\pm 2\%$ ) in sulfur hexafluoride were irradiated and allowed to stand for a definite time before analysis. The results, presented in Figure 5 and Table V, show the alcohol yield to

TABLE IV

n-Propanol Yield as a Function of Sulfur Hexafluoride Con-  
centration and Time Irradiated Sample Stood Before Analysis

$[SF_6]$ Molar	$G(1-C_3H_7OH)$	Approximate Time After Irradiation
$1.9 \times 10^{-3}$	1.55	5 mins
$6.5 \times 10^{-3}$	0.96	"
$7.7 \times 10^{-3}$	1.05	"
$3.8 \times 10^{-4}$	1.86	<5 hrs
$5.5 \times 10^{-4}$	1.83	"
$6.5 \times 10^{-4}$	1.79	"
$1.0 \times 10^{-3}$	1.49	"
$2.9 \times 10^{-3}$	0.82	"
$4.0 \times 10^{-3}$	0.91	"
$5.8 \times 10^{-3}$	0.77	"
$1.2 \times 10^{-2}$	0.81	"
$1.6 \times 10^{-2}$	0.56	"
$2.0 \times 10^{-2}$	0.58	"
$3.1 \times 10^{-1}$	0.21	"
$6.0 \times 10^{-1}$	0.19	"
$3.9 \times 10^{-3}$	0.32	15-20 hrs
$4.7 \times 10^{-3}$	0.46	"
$1.1 \times 10^{-2}$	0.47	"
$1.6 \times 10^{-2}$	0.21	"
$1.8 \times 10^{-1}$	0.09	"
$4.1 \times 10^{-1}$	0.11	"



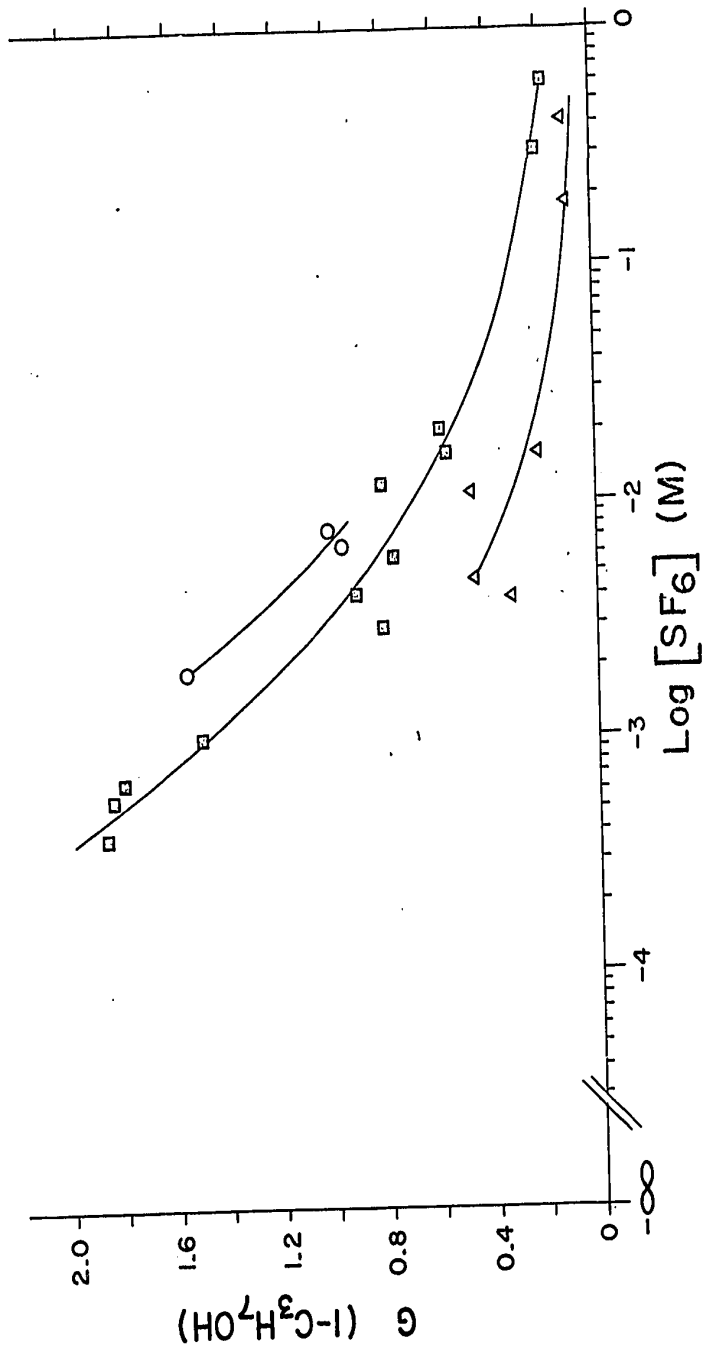


FIGURE 4. n-Propanol yield as a function of sulfur hexafluoride concentration and time irradiated sample stood before analysis.

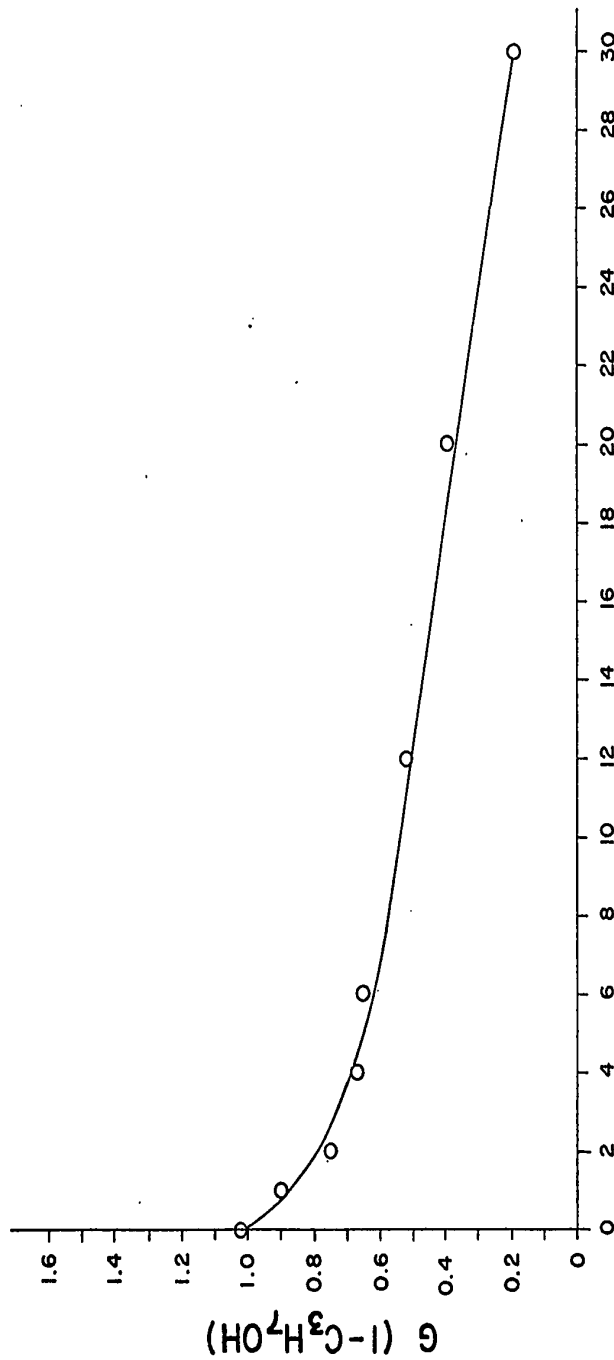
□, ~ 5 hrs; Δ, ~ 15-20 hrs.

TABLE V

n-Propanol Yield as a Function of Time Sample ( $9 \times 10^{-3}$  M SF<sub>6</sub>)  
Stood After Irradiation

<u>Time (Hours)</u>	<u>G(1-C<sub>3</sub>H<sub>7</sub>OH)</u>
0	1.02
1	0.90
2	0.75
4	0.67
6	0.65
12	0.52
20	0.39
30	0.19

---



**FIGURE 5.** Dependence of n-propanol yield on time irradiated sample stood before analysis.

decrease with time. One of the minor products of radiolysis of pure n-propyl ether was shown to be 1,1-dipropoxypropane by mass spectrometry. The concentration of this product was found to increase with time after irradiation.

3. The effect of concentration of sulfur hexafluoride was investigated, all samples being analysed immediately after irradiation. The concentrations of sulfur hexafluoride were calculated using the experimentally obtained  $\alpha = 1.70$ . The volume of the cell was measured at the conclusion of the analysis. The difference between the volume of the cell and the volume of the liquid ether was the volume occupied by the undissolved gas.

1,1-Dipropoxypropane was formed by an acid catalysed reaction of propionaldehyde with propanol. The acid was presumably hydrogen fluoride since the dipropoxypropane yield was enhanced by the presence of sulfur hexafluoride. Hence, the total propanol yield was expressed as

$$G(1-C_3H_7OH) = G(1-C_3H_7OH) + 2G[1,1-C_3H_6-(OC_3H_7)_2]$$

measured

The results are presented in Figure 6 and Table VI. The propanol and dipropoxypropane yields decrease with increasing concentration of sulfur hexafluoride. The total propanol yield decreased from 2.52 to 0.72 over the concentration range 0-1 M.

TABLE VI

Product Yields as a Function of Sulfur Hexafluoride Concentration

[SF <sub>6</sub> ] Molar	G(1-C <sub>3</sub> H <sub>6</sub> O)	G(1-C <sub>3</sub> H <sub>7</sub> OH)	G[1,1-C <sub>3</sub> H <sub>6</sub> (OC <sub>3</sub> H <sub>7</sub> ) <sub>2</sub> ]	G(1-C <sub>3</sub> H <sub>7</sub> OH)	G(1-C <sub>3</sub> H <sub>7</sub> OH)	G(1-C <sub>3</sub> H <sub>6</sub> (OC <sub>3</sub> H <sub>7</sub> ) <sub>2</sub> )	G(1-C <sub>3</sub> H <sub>7</sub> OH)	G(1-C <sub>3</sub> H <sub>6</sub> (OC <sub>3</sub> H <sub>7</sub> ) <sub>2</sub> )
		measured						
0.0	0.30	2.50	0.01	0.01	2.52			
4.3 x 10 <sup>-4</sup>		1.40	0.46	0.46	2.32			
7.8 x 10 <sup>-4</sup>		1.53	0.44	0.44	2.41			
4.0 x 10 <sup>-3</sup>		0.94	0.65	0.65	2.24			
4.5 x 10 <sup>-3</sup>		0.99	0.47	0.47	1.93			
7.9 x 10 <sup>-3</sup>		0.70	0.61	0.61	1.92			
9.9 x 10 <sup>-3</sup>		0.61	0.53	0.53	1.67			
2.1 x 10 <sup>-2</sup>		0.53	0.34	0.34	1.21			
3.8 x 10 <sup>-2</sup>		0.43	0.26	0.26	0.95			
8.5 x 10 <sup>-2</sup>		0.36	0.20	0.20	0.76			
1.4 x 10 <sup>-1</sup>		0.39	0.24	0.24	0.87			
7.5 x 10 <sup>-1</sup>		0.28	0.11	0.11	0.50			
8.5 x 10 <sup>-1</sup>		0.61	0.18	0.18	0.97			
1.0		0.47	0.14	0.14	0.75			

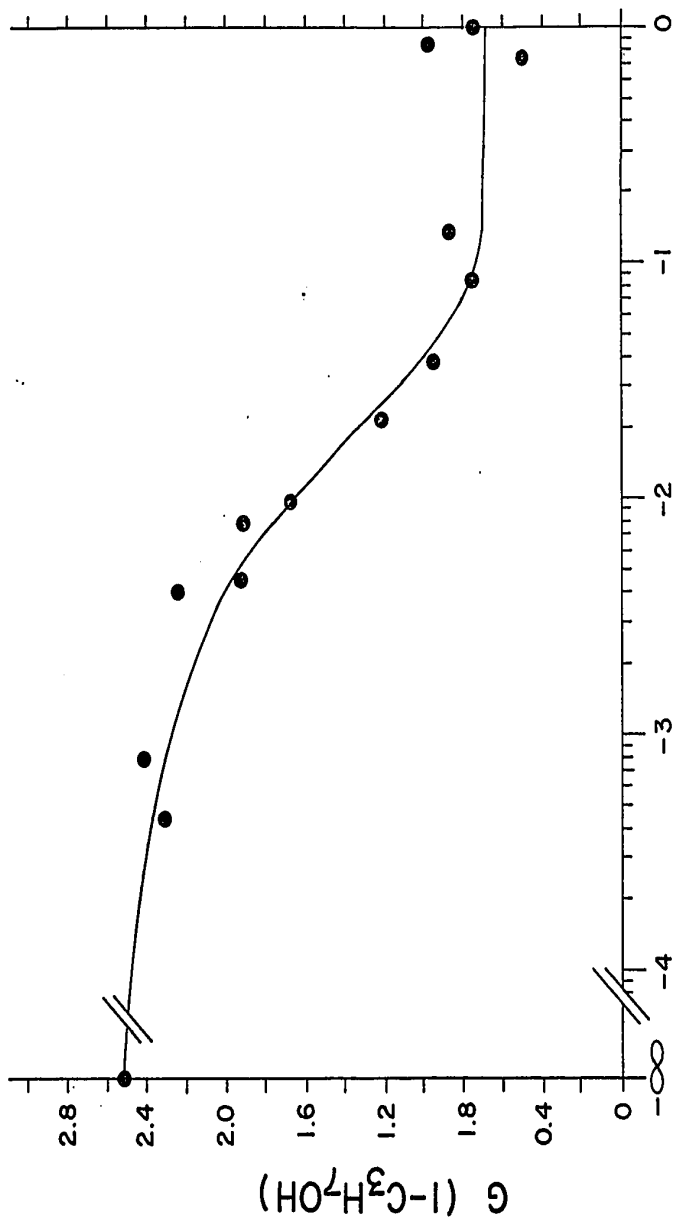


FIGURE 6. n-Propanol yield as a function of sulfur hexafluoride concentration. ●, experimental points. —, calculated from a statistical non-homogeneous kinetic model.

### Part III Ether-Hydrogen Chloride Solutions

The variation of product yields with hydrogen chloride concentration is presented in Figure 7 and Table VII. Throughout the concentration range studied, hydrogen chloride had no effect on the radiolysis yield of propanol. At concentrations above  $1 \times 10^{-1}$  M, the acid decomposition of ether to propanol and 1 and 2-propyl chloride was appreciable. The G values of propyl chlorides was subtracted from the measured G value of propanol to give the actual radiolysis yield.

### Part IV Ether-Sulfuric Acid Solutions

The study of the effect of sulfuric acid on propanol yield in irradiated ether was limited to two samples only. It was not necessary to continue the study after it was found that sulfuric acid decomposes the propyl ether to propanol and propyl hydrogen sulfate. Propanol was identified by its mass spectrum and by gas chromatography and the propyl hydrogen sulfate by its physical characteristics. Propyl hydrogen sulfate was obtained by adding about 5  $\mu$ l water to 1 cc of 1 M sulfuric acid in ether. Propyl hydrogen sulfate separated from the ether on standing. The liquid was colorless, acidic, denser than ether and very viscous. Unlike di-propyl sulfate, it was very soluble in water, less soluble in ether and decomposed on heating.

#### Part V Ether-n-Propylamine Solutions

The variation of propanol yield with n-propylamine is shown in Figure 8 and Table VIII. The amine decreased the propanol yield starting at around  $10^{-1}$ M. The higher yields of propanol in this series arose from a lesser tailing and sharper resolution of products on Porapak Q column.

#### Part VI Ether-Propylene Solutions

The results of propylene scavenging study are shown in Figure 9 and Table IX. No effect on alcohol yield was observed to 1 M concentration of propylene. A study at lower concentrations was deemed unnecessary for lack of effect at higher concentrations.



TABLE VIIProduct Yields as a Function of Hydrogen ChlorideConcentration

<u>[HCl] Molar</u>	<u>G(1-C<sub>3</sub>H<sub>7</sub>OH)</u>	<u>G(1-C<sub>3</sub>H<sub>7</sub>Cl + 2-C<sub>3</sub>H<sub>7</sub>Cl)</u>
0	2.52	
4.5 x 10 <sup>-3</sup>	2.54	
9.1 x 10 <sup>-3</sup>	2.41	
1.8 x 10 <sup>-2</sup>	2.43	
6.1 x 10 <sup>-1</sup>	2.87	0.43
8.3 x 10 <sup>-1</sup>	2.48	1.07
8.7 x 10 <sup>-1</sup>	2.86	1.08
1.0	3.10	1.02

---

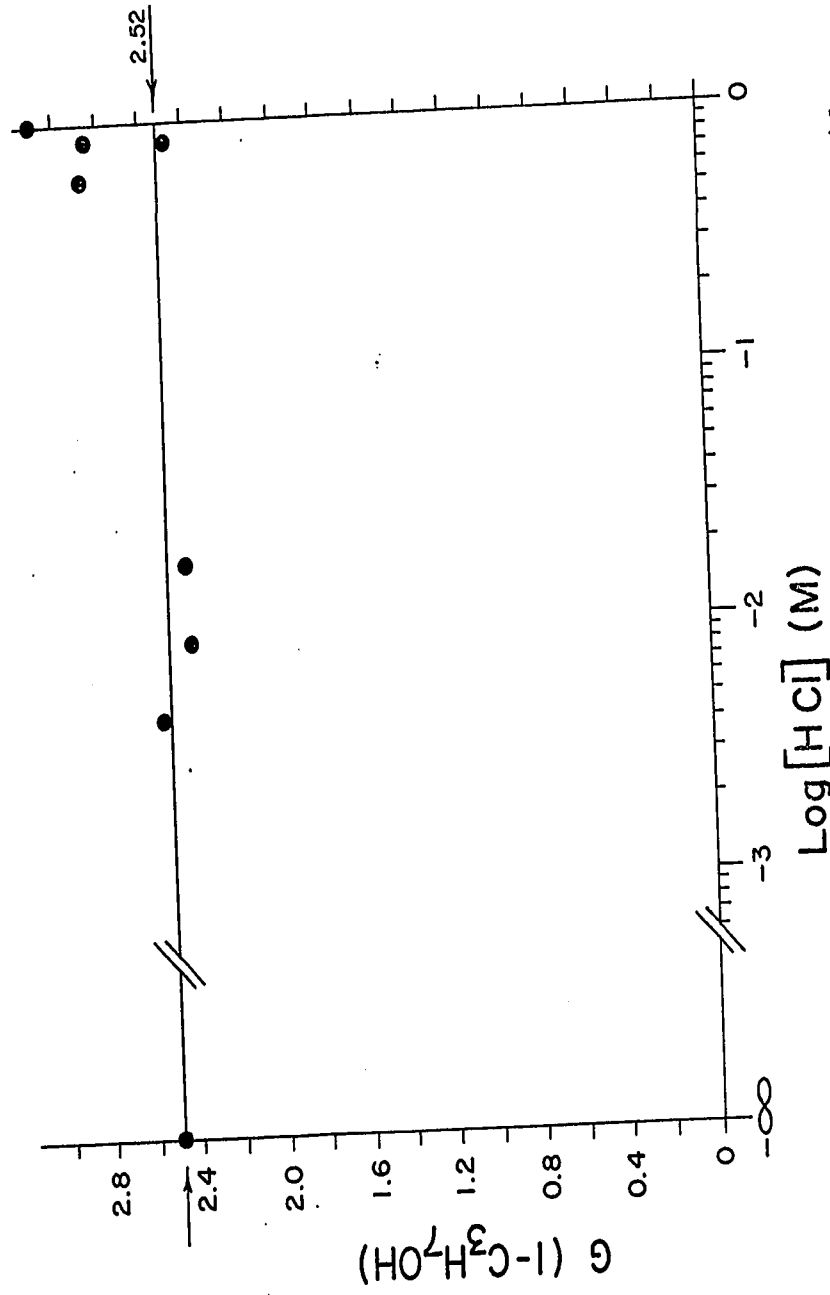


FIGURE 7. n-Propanol yield as a function of hydrogen chloride concentration.

TABLE VIIIn-Propanol Yield as a Function of n-PropylamineConcentration

<u>[1-C<sub>3</sub>H<sub>7</sub>NH<sub>2</sub>] Molar</u>	<u>G(1-C<sub>3</sub>H<sub>7</sub>OH)</u>
0	2.64
1.1 x 10 <sup>-3</sup>	2.70
9.4 x 10 <sup>-3</sup>	2.69
2.4 x 10 <sup>-2</sup>	2.65
5.1 x 10 <sup>-2</sup>	2.51
1.0 x 10 <sup>-1</sup>	2.40
1.0 x 10 <sup>-1</sup>	2.34
4.8 x 10 <sup>-1</sup>	2.0
9.3 x 10 <sup>-1</sup>	1.68

---

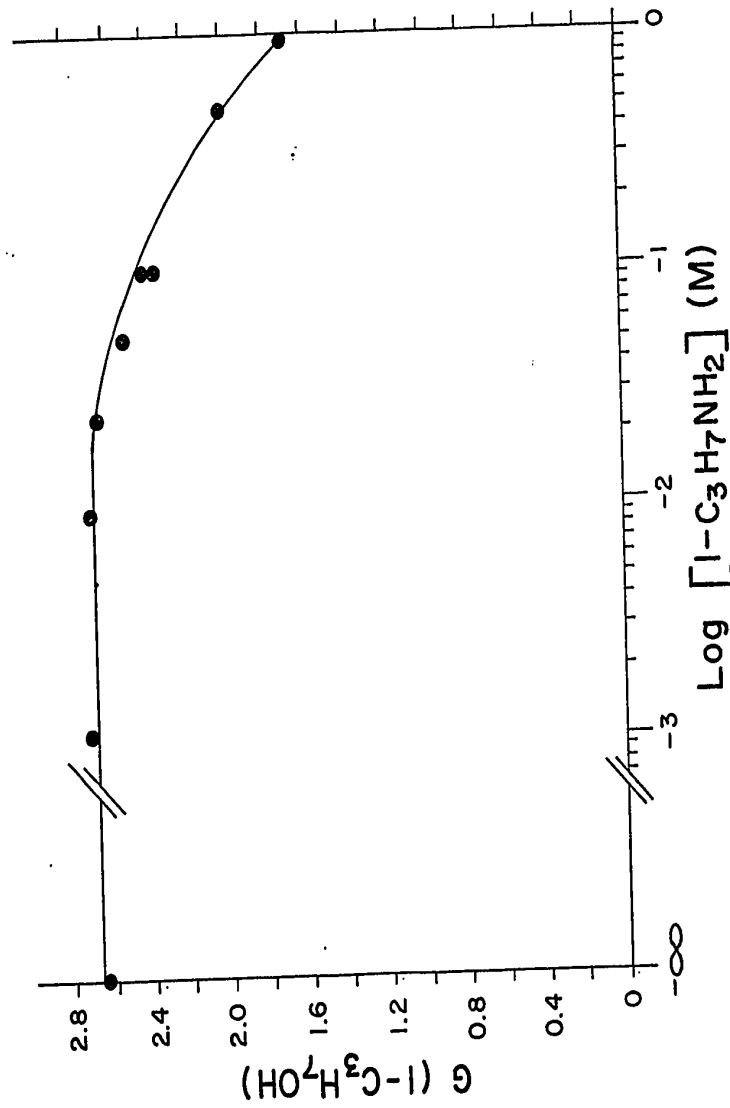


FIGURE 8. n-Propanol yield as a function of n-propylamine concentration.

TABLE IXn-Propanol Yield as a Function of Propylene  
Concentration

<u>[C<sub>3</sub>H<sub>6</sub>] Molar</u>	<u>G(1-C<sub>3</sub>H<sub>7</sub>OH)</u>
0	2.52
9.3 x 10 <sup>-3</sup>	2.58
5.4 x 10 <sup>-2</sup>	2.52
1.1 x 10 <sup>-1</sup>	2.42
2.3 x 10 <sup>-1</sup>	2.41
5.0 x 10 <sup>-1</sup>	2.49
1.0	2.49

---

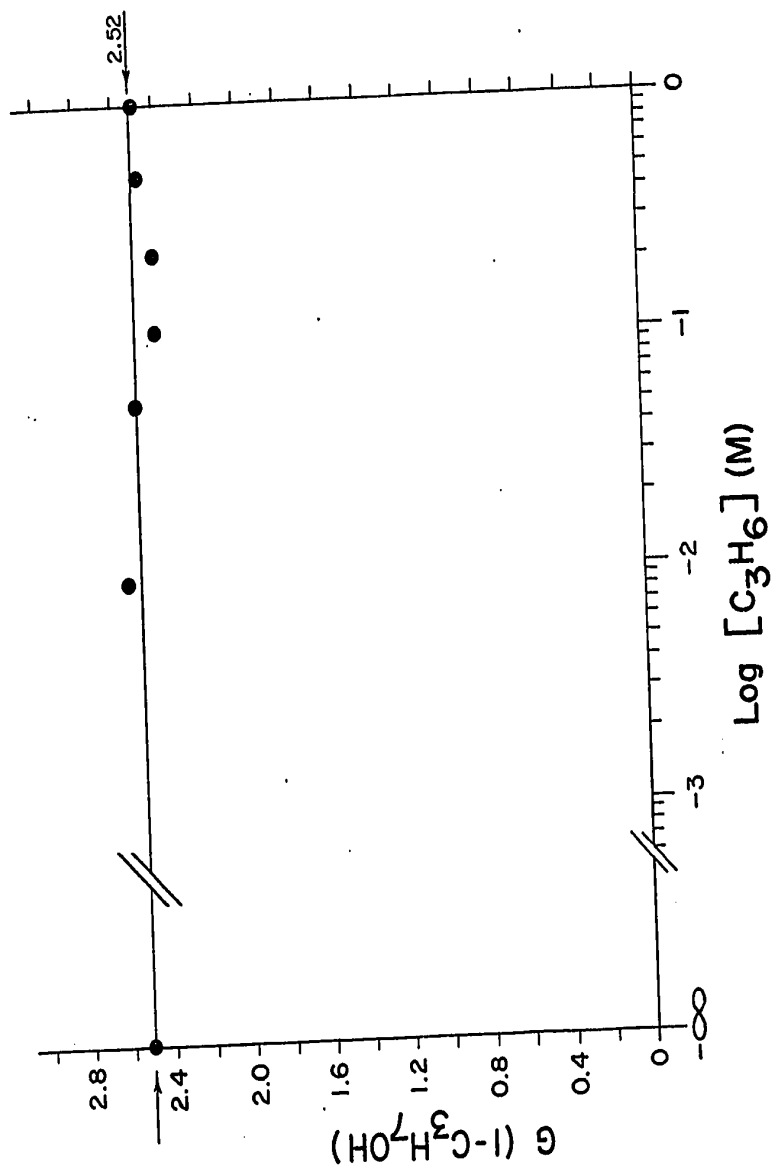


FIGURE 9. n-Propanol yield as a function of propylene concentration.

### III PULSE RADIOLYSIS OF n-PROPYL ETHER

Evidence for the presence of solvated electrons in the radiolysis of liquid n-propyl ether has been obtained through scavenging studies. A direct observation of these reactive species would provide a confirmation for its existence in the radiolysis of n-propyl ether. The pulse radiolysis technique allows the direct observation of solvated electron through its absorption spectrum and its half-life in a given reaction. In the pulse radiolysis experiments described below, the absorption spectrum of solvated electron, its half-life with respect to its reaction in ether and with sulfur hexafluoride were determined at various temperatures.

#### A Experimental

##### Part I. The Pulse Radiolysis Experiment

The apparatus used in electron absorption signal measurement is presented in Figure 10. The solvated electrons, generated by irradiation of a medium with a pulsed electron beam, absorb light. The transient absorption is recorded as a function of time with a photodetector set at an appropriate wavelength.

To protect a sample from photolysis and heating, the light beam was interrupted by a shutter. The shutter was operated by a push button in the control room. When

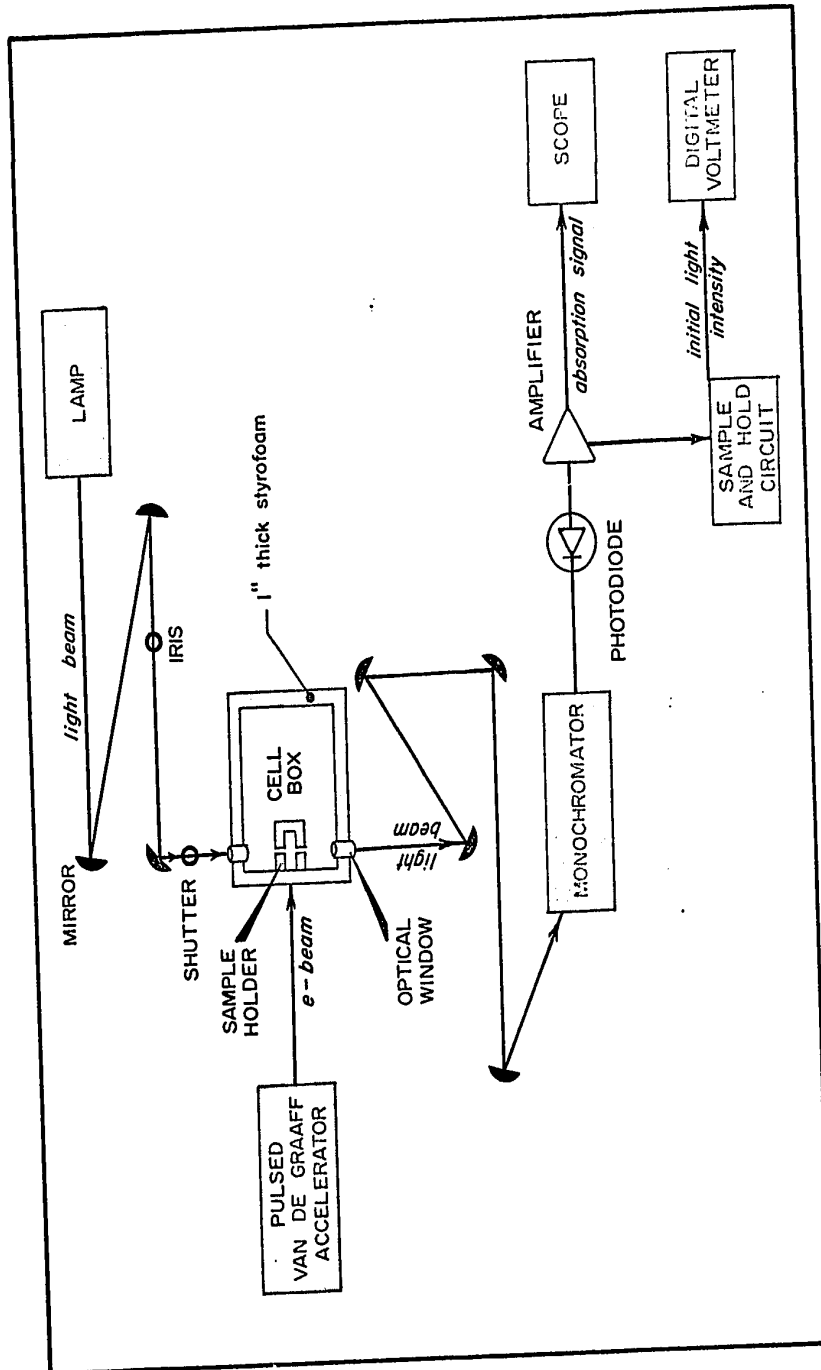


Figure 10 : PULSE RADIOLYSIS EQUIPMENT



the shutter was opened, the light from a constant intensity Xenon lamp was passed through the sample cell by a system of aluminum mirrors. The light was then passed through a monochromator and a selected wavelength directed to the photodiode. With the shutter opened, triggering signals were sent to the accelerator to trigger a beam pulse and to the photodiode to measure the initial light intensity. The photodiode signal was amplified and read on the digital voltmeter. The initial light intensity was measured 50 - 100  $\mu$ sec before the beam pulse hit the sample.

When the beam hit the sample, the build-up in solvated electron concentration and its decay was measured by the photodiode as a transient decrease in light signal. The absorption signal was introduced into an oscilloscope and the trace corresponding to the transient absorption was photographed with a Polaroid camera. In the simplest arrangement, the absorption signal would arrive at the oscilloscope about 35  $\mu$ sec earlier than the signal that triggered the scope to scan (see Figure 10). In order to give time for the scope to begin its sweep prior to the arrival of the absorption signal the latter was passed through a delay circuit within the scope.

## Part II    Components of the Pulse Radiolysis Apparatus

### (1) Van de Graaff Accelerator

The van de Graaff is an electrostatic accelerator

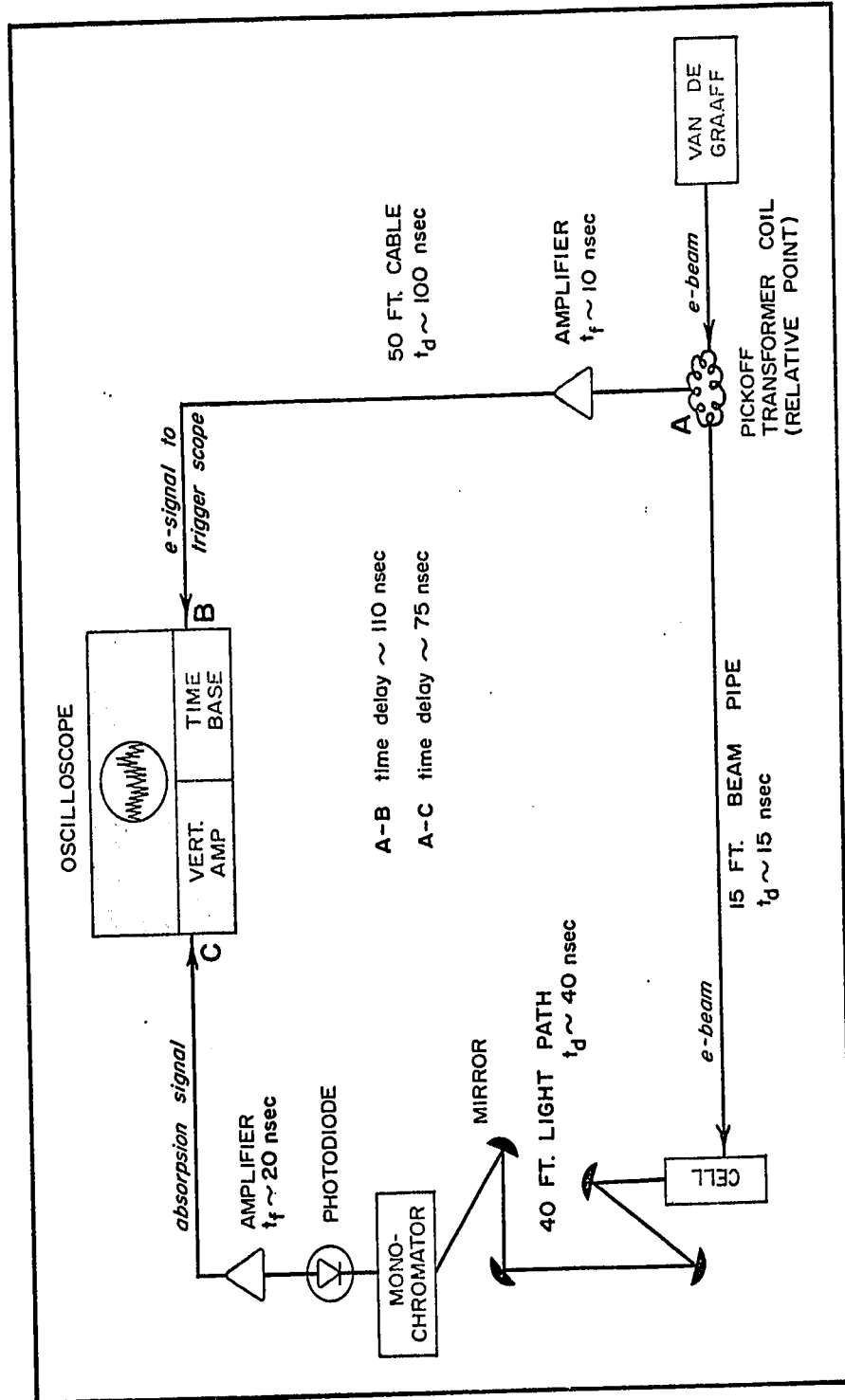


Figure II : TIME DELAY FOR ABSORPTION SIGNAL AND ELECTRON SIGNAL

that can deliver either a DC beam or a pulsed beam. The electron pulse current has a range of 10 - 100 mA. The time duration of the pulses can be 3 nsec, 10 nsec, 30 nsec, 100 nsec, 1  $\mu$ sec or variable milliseconds. The energy range of the beam is 0.7 - 2.0 MeV and the energy stability is 0.2%.

(2) Lamp

A 450 watt High Pressure Xenon Arc Lamp was used.

(3) Cell-Temperature System

A styrofoam box that held the cell was cooled by evaporating liquid nitrogen and blowing the cold gas through the box. The temperature of the box and that of the sample cell was automatically controlled by the API Instrument 2-Mode Controller. The automatic temperature controller powered a 1000 watt Nichrome heater which boiled the nitrogen. The cold vapor was channeled from a 50 liter Dewar to the cell box in a styrofoam insulated copper pipe. The temperature was constant within  $\pm 1^\circ\text{C}$ .

(4) Cell

The cell consisted of a rectangular optical cell of high purity silica (Spectrosil) measuring 1 x 1 x 4.5 cm and a Pyrex side arm bulb with a volume of about 8 cc. The surface of the cell window facing the beam was thinned by grinding. The sample was condensed into the

Pyrex bulb and transferred to the optical cell after it was sealed off. The temperature of the cell was monitored by a copper-constantan thermocouple attached to a cell window.

(5) Monochromator

The monochromators used were Bausch and Lomb Visible grating and Infrared grating monochromators which covered the region 350-800 nanometers and 700-1600 nanometers, respectively.

(6) Filters

The types of filters used were:

- (a) Corning Filter #3-74 - a clear glass filter with cut-off below 400 nm to clear the 400-800 nm region of higher order diffractions from the region below 400 nm.
- (b) Corning Filter #3-66 - an orange glass filter with cut-off below 560 nm to clear the region 560-1120 nm of higher order diffraction from the region below 560 nm.
- (c) Corning Filter #7-56 - a violet glass filter with cut-off below 800 nm to clear the 800-1600 nm region of higher order diffractions from the region below 800 nm.

(7) Calibrating Laser

The light used to calibrate the grating monochromators was a He-Ne laser, University Laboratories Model 240,  $\lambda = 6328 \text{ \AA}$ . The first order  $\lambda = 6328 \text{ \AA}$  and the second order  $\lambda = 12656 \text{ \AA}$  were used to calibrate the visible and infrared grating respectively.

(8) Photodetectors

A silicone photodiode EG & G Model SGD444 was used as a visible detector and a germanium optical detector ENL Type 653 as an infrared detector.

The absorption spectra were followed with a visible-light detector from 400-1000 nm and with an infrared detector from 700-1000 nm. The visible-light detector response fell off at 1000 nm while that of the infrared detector fell off at 1700 nm. As compared to the visible-light detector, the infrared detector had a slower response time and therefore gave smaller absorption peak heights. At temperatures  $0^\circ$  and  $-133^\circ\text{C}$ , the % absorption/ncoul SEM from the region 700-1000 nm registered by the infrared detector was 0.581 times that registered by the visible detector. To get a continuous absorption spectrum from 400-1600 nm at  $0^\circ$  and  $-133^\circ\text{C}$ , the % absorption/ncoul SEM obtained with the visible-light detector was normalized by a factor of 0.581. At  $-73^\circ\text{C}$ , the % absorption/ncoul SEM registered by both detectors was the same over the

700-1000 nm region so the normalization factor was unity.

(9) Absorption Amplifier

The amplifier used was a non-commercial amplifier which separated the absorption signal from the initial light signal and had an amplification ratio of 5.7/1. The rise time and fall time were equal and were less than 35 nsec.

(10) Oscilloscope

Two types of oscilloscopes were used, depending on the lifetime of the transient absorption. A Tektronix 549 Storage Scope was used to display absorption signals with  $t_{1/2} \geq 1 \mu\text{sec}$  and a Tektronix 7704 High Speed Scope for signals with  $t_{1/2} < 1 \mu\text{sec}$ .

(11) Camera

A Tektronix Model C12 Polaroid camera was used to photograph scope traces. The polaroid films used were Type 47 speed 3000 ASA with the storage scope and Type 410 speed 10,000 ASA with the high speed scope.

(12) Digital Voltmeter

A Hewlett-Packard Digital Voltmeter Model 3440-A was used to display the initial light intensity measurement.

(13) SEM

The dose absorbed per pulse by the sample was monitored

as a relative dose by the Secondary Emission Monitor (SEM). Figure 12 illustrates the 3-foil SEM used with the van de Graaff accelerator. The secondary electrons generated by impact of the electron beam on the aluminum foils are collected by a central electrode. The current arising from the secondary electrons is called the SEM current. The SEM monitors the beam current. When calibrated against the beam current, the SEM current is found to be about 5% of the beam current. When calibrated by a dosimeter placed at an irradiation field point, it becomes a dose monitor. The dose at the irradiation point is about  $5 \times 10^{16}$  eV/ml of water per nanocoulomb registered by the SEM.

In the experiments performed, the absolute dose information was not required and, since only a normalizing factor was needed, the SEM current per 1  $\mu$ sec pulse duration (SEM nanocoulomb) was used as a relative dose to normalize the % absorption per pulse at a given wavelength in the determination of the absorption spectrum.

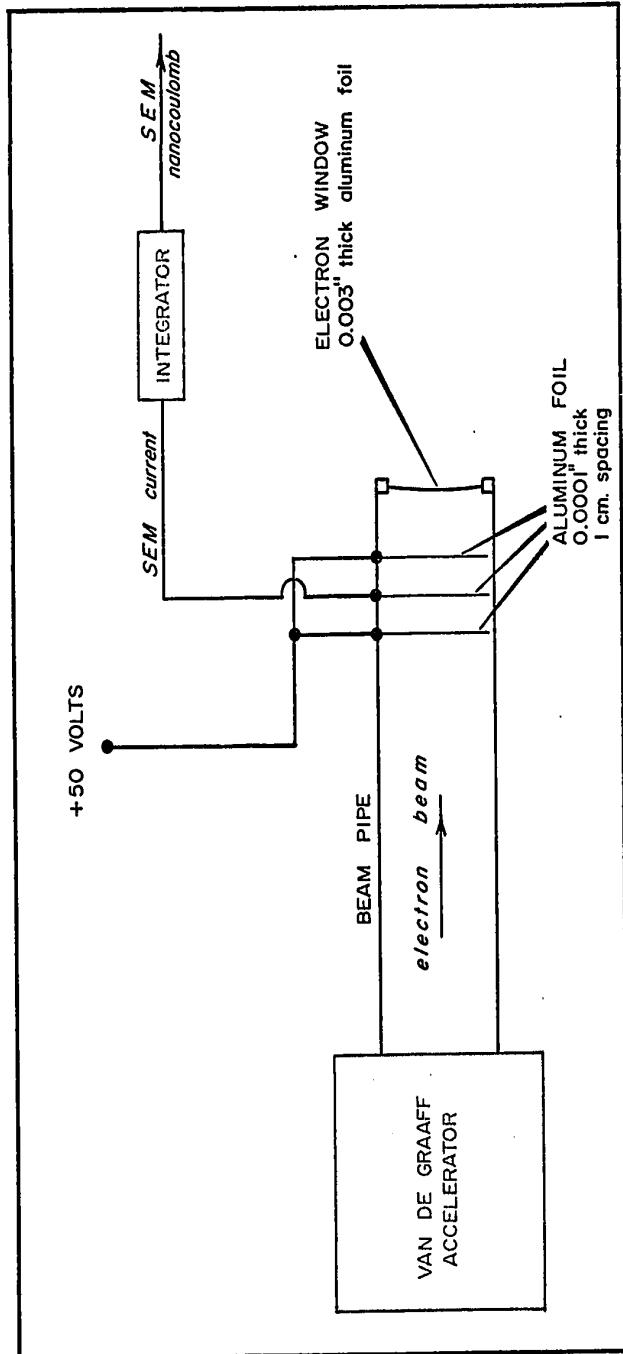


Figure 12 : SECONDARY EMISSION MONITOR (SEM)



## B. Results

### Part I Absorption Spectra of Solvated Electrons

The absorption spectra of solvated electrons in n-propyl ether at temperatures 0°, -73° and -133°C are shown in Figure 13. At -133°C, the ether was in the supercooled state. At all three temperatures, the absorption maxima lay above 1600 nm. The change in the shape of the spectrum with temperature (Figure 13) indicates a shift of the absorption maximum to shorter wavelengths at lower temperatures. Superimposed on the absorption spectrum of ether at -133°C (Figure 13) is the partial absorption spectrum of ether which had been made  $1.1 \times 10^{-4}$  M in sulfur hexafluoride. Although the spectrum shows no change in shape as compared to the spectrum in pure ether, the half-life of the solvated electrons was decreased by sulfur hexafluoride.

### Part II Order of Reaction, Half-life and Rate Constant

The order of reaction, half-life and rate constant of the reaction of solvated electrons at various temperatures in n-propyl ether and in solutions of sulfur hexafluoride are presented in Table X. Representative absorption signals from which the half-life and order of reaction were determined are given in Figures 14A-14C. The plots of reaction order for the decay of solvated

TABLE X

Order of Reaction, Half-life and Rate Constants of Solvated Electron Reactions

	Order of Reaction	$t_{1/2}$ (1st order tail)	$k_1$ ( $e^-$ solv)	$k_2$ ( $e^-$ solv + SF <sub>6</sub> )
<u>0°C</u>				
n-Propyl ether	1st order	0.80 μsec	8.7 x 10 <sup>5</sup> sec <sup>-1</sup>	
1.9 x 10 <sup>-5</sup> M SF <sub>6</sub>	1st order	0.45 μsec		4.5 x 10 <sup>10</sup> M <sup>-1</sup> sec <sup>-1</sup> (+0.8)
2.7 x 10 <sup>-5</sup> M	1st order	0.30 μsec		
<u>-73°C</u>				
n-Propyl ether	2nd+1st*	12.8 μsec	5.4 x 10 <sup>4</sup> sec <sup>-1</sup>	
5.1 x 10 <sup>-5</sup> M SF <sub>6</sub>	1st order	1.2 μsec		1.05 x 10 <sup>10</sup> M <sup>-1</sup> sec <sup>-1</sup> (+0.05)
1.1 x 10 <sup>-4</sup> M SF <sub>6</sub>	1st order	0.55 μsec		
<u>-124°C</u>				
n-Propyl ether	2nd+1st	70 μsec	9.9 x 10 <sup>3</sup> sec <sup>-1</sup>	
<u>-133°C</u>				
n-Propyl ether	2nd+1st	>70 μsec		
3.7 x 10 <sup>-4</sup> M SF <sub>6</sub>	2nd+1st	11.3 μsec		1.3 x 10 <sup>8</sup> M <sup>-1</sup> sec <sup>-1</sup> (+0.1)
5.3 x 10 <sup>-4</sup> M SF <sub>6</sub>	2nd+1st	9.5 μsec		

\* 2nd+1st is a notation that the order of reaction proceeded from an order higher than first going to first order at long times.

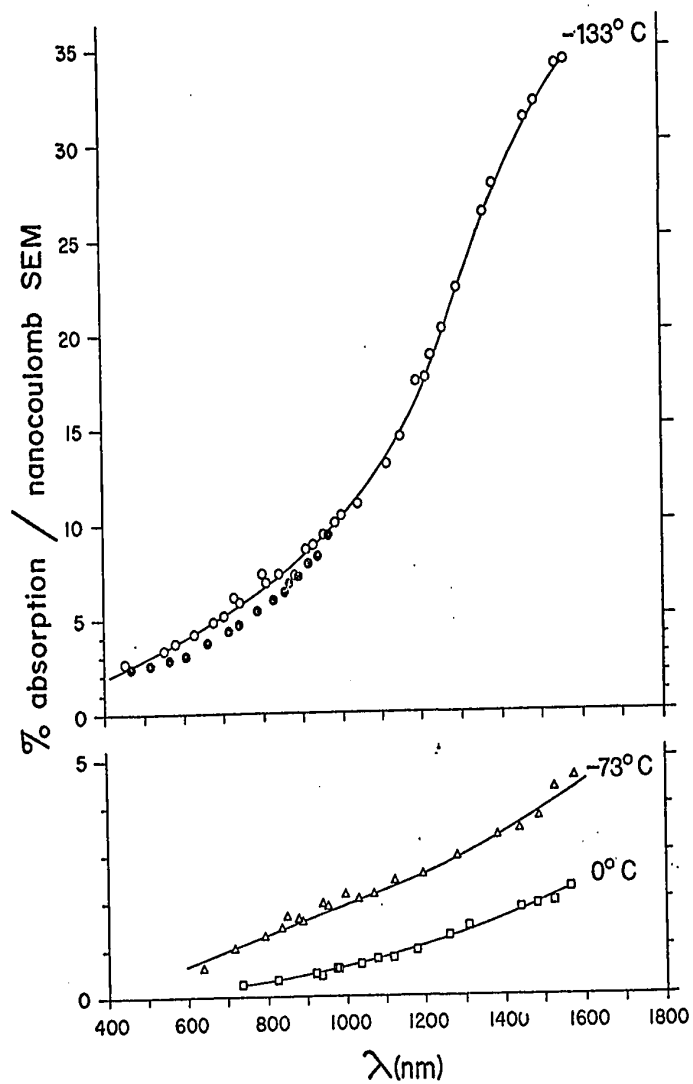


FIGURE 13. Absorption spectra of solvated electrons. O,  $-133^\circ\text{C}$  n-propyl ether;  $\bullet$ ,  $-133^\circ\text{C}$ ,  $1.1 \times 10^{-4}$  M sulfur hexafluoride;  $\Delta$ ,  $-73^\circ\text{C}$ , n-propyl ether;  $\square$ ,  $0^\circ\text{C}$ , n-propyl ether.

0°C

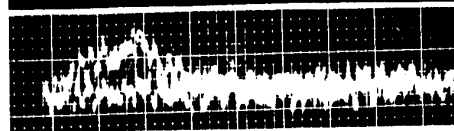
n-Propyl Ether  
 $\lambda = 859 \text{ nm}$   
 time base =  $0.5 \mu\text{sec/cm}$



$1.9 \times 10^{-5} \text{ M SF}_6$   
 $\lambda = 901 \text{ nm}$   
 time base =  $0.5 \mu\text{sec/cm}$

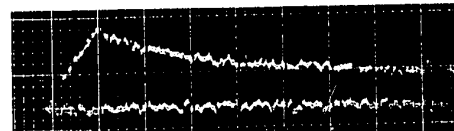


$2.7 \times 10^{-5} \text{ M SF}_6$   
 $\lambda = 901 \text{ nm}$   
 time base =  $0.5 \mu\text{sec/cm}$

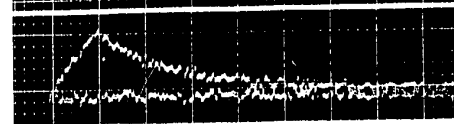


-73°C

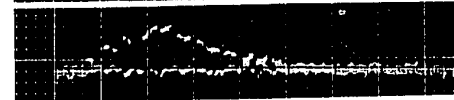
n-Propyl Ether  
 $\lambda = 906 \text{ nm}$   
 time base =  $1 \mu\text{sec/cm}$



$5.1 \times 10^{-5} \text{ M SF}_6$   
 $\lambda = 917 \text{ nm}$   
 time base =  $1 \mu\text{sec/cm}$

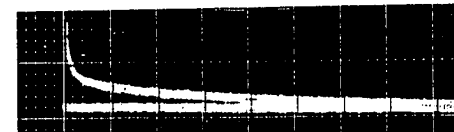


$1.1 \times 10^{-4} \text{ M SF}_6$   
 $\lambda = 904 \text{ nm}$   
 time base =  $0.5 \mu\text{sec/cm}$



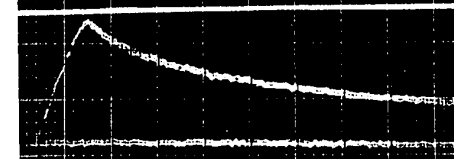
-124°C

n-Propyl Ether  
 $\lambda = 900 \text{ nm}$   
 time base =  $20 \mu\text{sec/cm}$



-133°C

$3.7 \times 10^{-4} \text{ M SF}_6$   
 $\lambda = 824 \text{ nm}$   
 time base =  $1 \mu\text{sec/cm}$



-133°C

$5.3 \times 10^{-4} \text{ M SF}_6$   
 $\lambda = 870 \text{ nm}$   
 time base =  $1 \mu\text{sec/cm}$

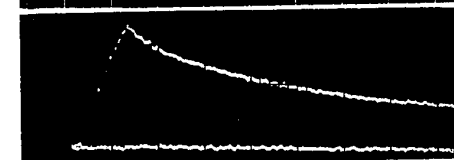


FIGURE 14 Representative Absorption Signals

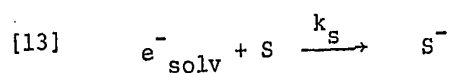
electrons are shown in Figures 15A-15C. The order of reaction was determined by plotting the  $\log(\text{mm})$  vs time and  $\frac{1}{\text{mm}}$  vs time, where (mm) represents the signal height in millimeters on the oscilloscope screen which is directly proportional to the concentration of solvated electrons. In certain cases (see for example Figure 15C), the order of the reaction is greater than one at short times and is unity at longer times. The order of reaction in these cases is denoted 2nd+1st. The half-life ( $t_{1/2}$ ) for a 1st order reaction was read directly from the photographed trace while for a 2nd+1st order reaction, the  $t_{1/2}$  was determined from the tail portion of the trace which showed 1st order decay. The rate constant  $k_2$  for the reaction of solvated electrons with sulfur hexafluoride was calculated using the equation:

$$[\text{ii}] \quad \frac{0.693}{t_{1/2}(\text{observed})} = \frac{0.693}{t_{1/2}(\text{pure ether})} + k_2[\text{SF}_6]$$

The rate constant  $k_1$  for the decay of solvated electrons in "pure" ether was calculated from the equation:

$$[\text{iii}] \quad k_1 = \frac{0.693}{t_{1/2}}$$

The decay of solvated electrons in "pure" ether is believed to be the bimolecular reaction



0°C

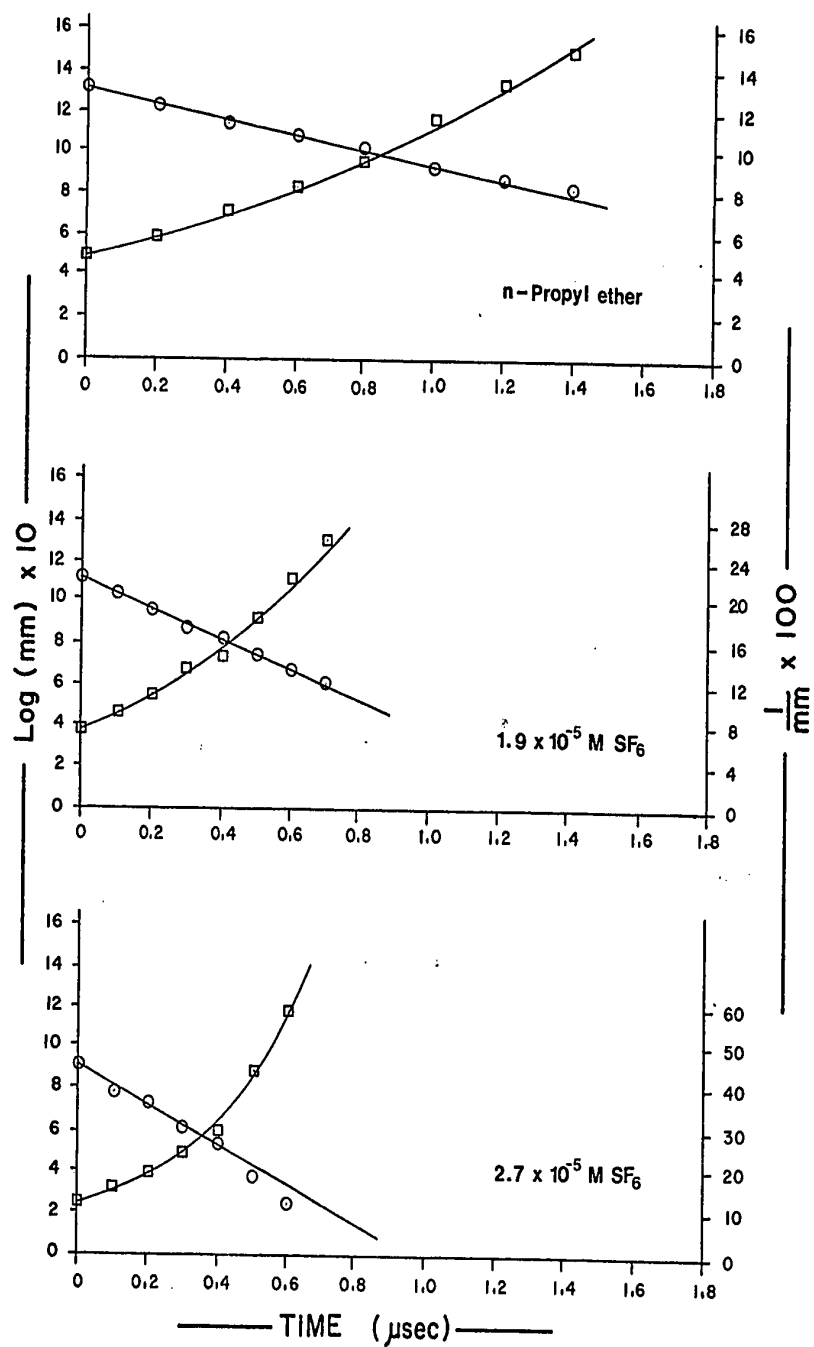


FIGURE 15A. Plots of Reaction Order. O, First order plot. □, Second order plot.

-73° C

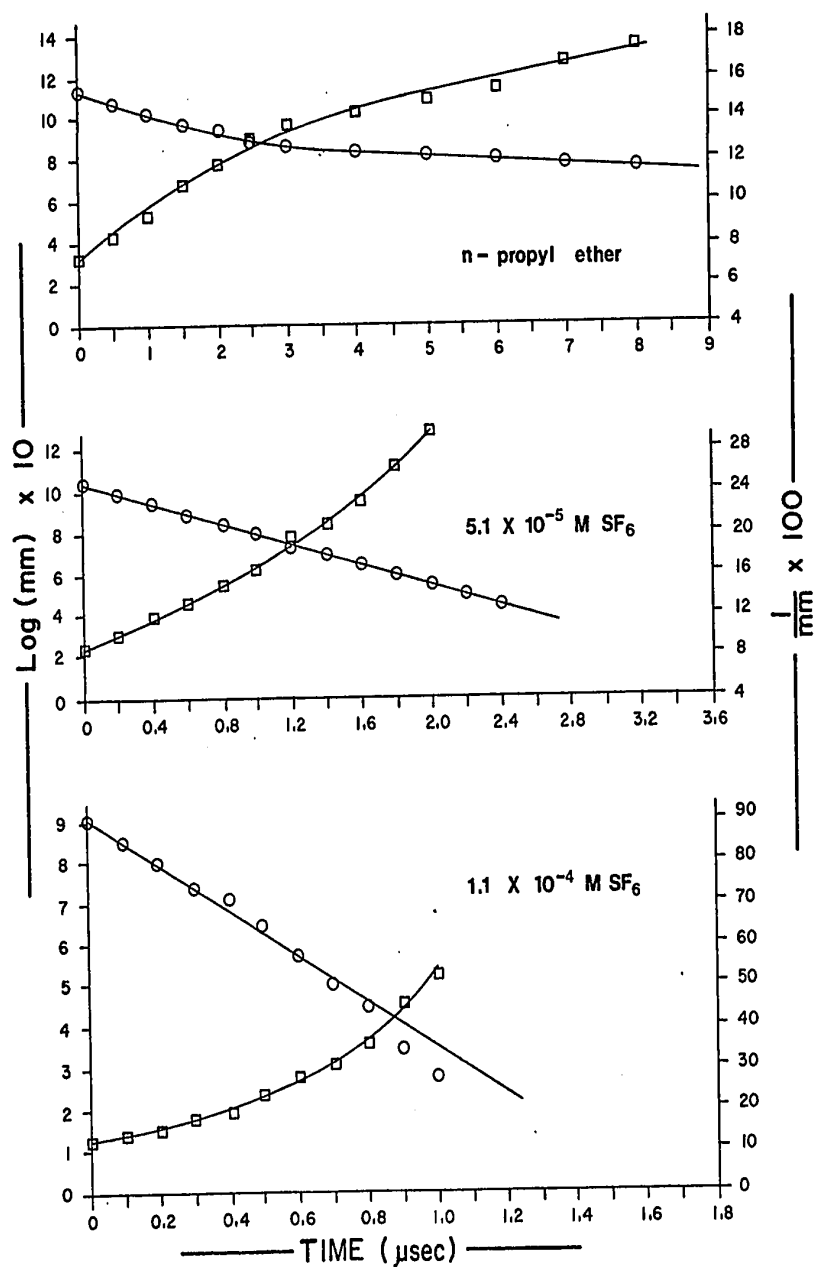


FIGURE 15B. Plots of Reaction Order. O, First order plot.  
 □, Second order plot.

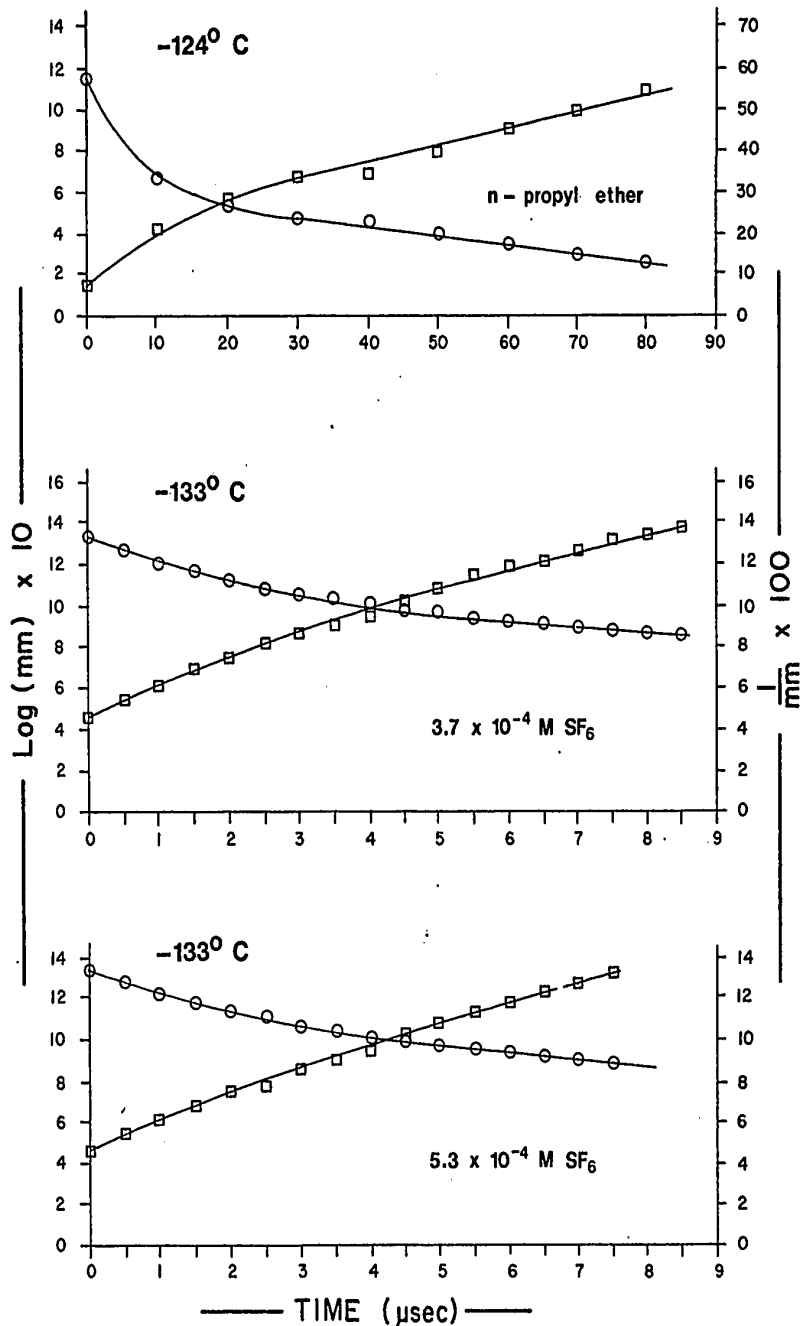


FIGURE 15C. Plots of Reaction Order. O, First order plot.  
 □, Second order plot.



where S is an impurity and  $k_s$  is the rate constant. The reaction was treated as pseudo-first order, thus the rate constant  $k_1$  is equal to  $k_s [S]$ .

At 0°C, the reaction of solvated electrons in ether was first order. At lower temperature, the reaction shifted towards higher order. A similar behavior was observed with the reaction of solvated electrons with sulfur hexafluoride. At 0° and -73°C, the reaction was first order and at -133°C, the order of the reaction was somewhat greater than first at short times.

### III Activation Energy ( $E_a$ )

The Arrhenius plot of the rate constant (Table X) for the reaction of solvated electrons with sulfur hexafluoride and in ether is shown in Figure 16. The slope of a line is equal to  $\frac{-E_a}{2.3R}$ , where  $R = 2 \text{ cal/deg.mole}$ . The activation energy for the reactions  $e^-_{\text{solv}} + S + S^-$  and  $e^-_{\text{solv}} + SF_6 + SF_6^-$  were found to be similar and equal to  $3 \pm 1 \text{ kcal/mole}$ .

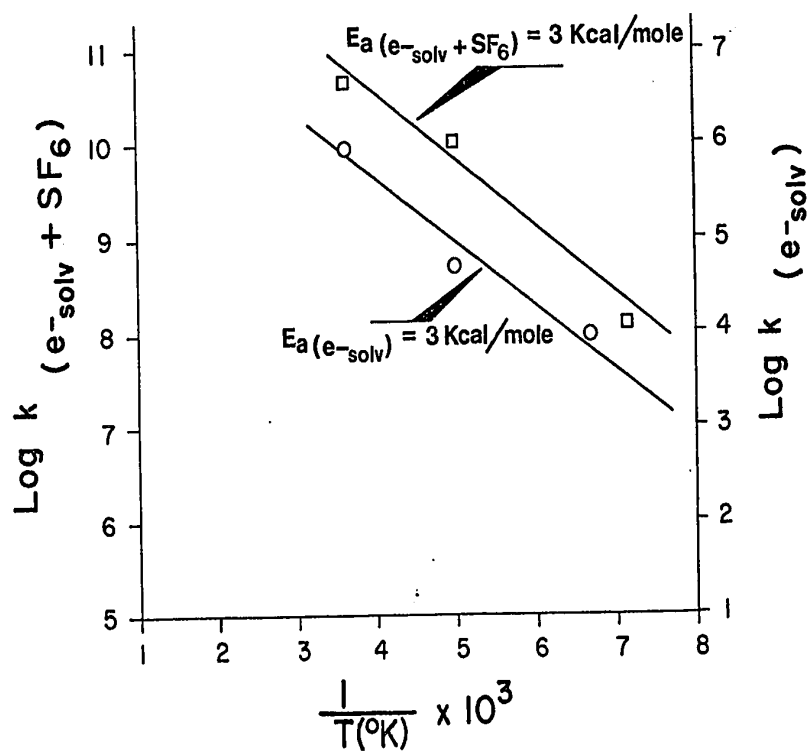
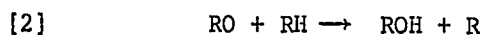


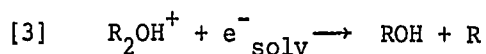
FIGURE 16. Arrhenius plot for rate constants of  $e^-_{\text{solv}}$  reactions.

IV D I S C U S S I O N

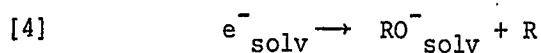
During the radiolysis of ether in the liquid phase, alcohol is among the major products formed. This was observed during the  $\text{He}^{+2}$  radiolysis of some aliphatic ethers (1). The mechanism of product formation during  $\gamma$  radiolysis of diethyl ether in the liquid phase was investigated by Ng (2). It was found that only about half the ethanol yield was scavengeable by 1,3-pentadiene. Being a conjugated di-olefin, 1,3-pentadiene could scavenge either free radicals (3) or electrons (4). Thus, the mechanism proposed for the scavengeable yield of alcohol was either the free radical reaction



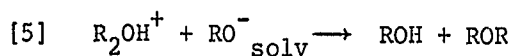
or a neutralization reaction



An alternative reaction of solvated electrons which could lead to alcohol formation is the decomposition reaction

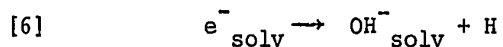


followed by

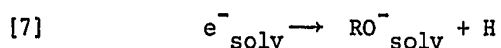


Reaction [4] is similar to the decomposition reaction of

solvated electrons which occurs in water



and in alcohols



The first order half-life for the decomposition reaction in water is 0.8 milliseconds, while in alcohols it is of the order of microseconds (5).

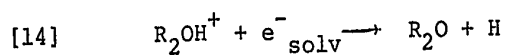
The study of the mechanism of alcohol formation in ether will provide evidence as to whether the decomposition reaction of solvated electrons which had been established in water and in alcohols, occurs in ether.

#### A. Mechanism

The mechanism of propanol formation in the  $\gamma$  radiolysis of di-n-propyl ether is elucidated by scavenging studies. The addition of sulfur hexafluoride, an electron scavenger, to the ether decreased the yield of propanol. It is seen from Figure 6 that nearly three-quarters of the alcohol yield is scavengeable by sulfur hexafluoride. This indicates that for about 1.8 G units of alcohol, solvated electrons are one of the precursors.

Figure 7 shows the effect of hydrogen chloride on the propanol yield. The acid was added with the purpose of obtaining information as to whether reaction [3] or [5]

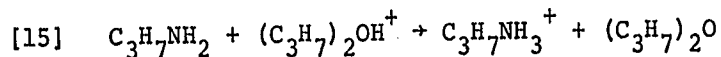
is the source of the scavengeable alcohol yield. The addition of the acid was expected to increase the concentration of the protonated ether ion  $R_2OH^+$ . If the alcohol was formed by reaction [3] the alcohol yield would remain the same. The higher concentration of  $R_2OH^+$  would only decrease the lifetime of solvated electrons in reaction [3]. If alcohol was formed by reaction [5] and not by [3], the yield would go down with increasing concentration of the acid since the protonated ether ion would scavenge the solvated electron precursor of  $RO^-$  by a reaction which did not produce alcohol. Such a scavenging reaction would be



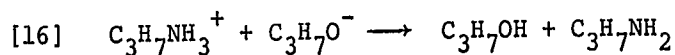
The addition of the acid was found to have no effect on the yield of propanol, lending support to reaction [3] as the source of scavengeable alcohol.

When n-propylamine, a positive ion scavenger, was added to the ether, the propanol yield decreased (Figure 8). From this it is deduced that a positive ion is a precursor of alcohol. The identity of the positive ion is proposed to be the protonated ether,  $(C_3H_7)_2OH^+$ . The amine scavenging study provided further evidence as to whether reaction [3] or [5] is the source of scavengeable propanol. If  $RO^-$  had been the precursor of alcohol, the alcohol yield would not have been affected by the addition of n-

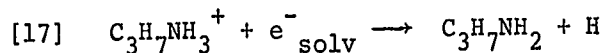
propylamine. The reactions would be



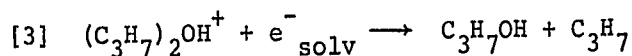
followed by



The reactions suggested by the scavenging effect of the amine are [15] followed by [17].

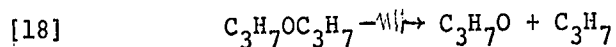


The hydrogen chloride and n-propylamine scavenging studies support the reaction

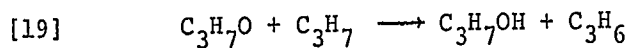


as the source of scavengeable propanol. As reaction [5] is ruled out by both studies, so is reaction [4].

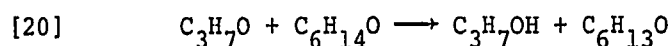
Based on the experimental data, a probable mechanism for the formation of scavengeable propanol has been postulated. No experimental evidence was obtained for the mechanism of the unscavengeable yield. However, probable mechanisms proposed for the unscavengeable yield are:



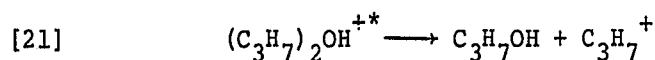
followed by disproportionation reaction



or H-atom abstraction

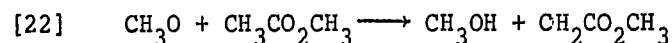


Another possible mechanism is the decomposition of the excited positive ion



Disproportionation reaction [19] would take place in a cage formed by the surrounding ether molecules. This reaction would occur in  $\sim 10^{-12}$  sec if the radicals have collision efficiencies near unity since collision frequencies in liquid cages are  $\sim 10^{13}$  sec $^{-1}$  (24b). Scavenging of the radicals in the cage would not occur.

The H-atom abstraction reaction [20] is a relatively slow reaction as indicated by the rate constants of the reaction of  $\text{CH}_3\text{O}$  with some molecules (36). For example, the reaction



has a rate constant  $k_{182^\circ\text{C}} = 3 \times 10^4 \text{ M}^{-1} \text{ sec}^{-1}$ . There has been no quantitative kinetic data on the addition of alkoxy radicals to olefins, from which rate constants could be calculated. Thus, it is not possible to evaluate whether the nonscavenging effect of propylene on the propanol yield (Figure 9) is due to the inability of propylene to compete

with reaction [20] or that reaction [20] does not take place at all.

The decomposition reaction [21] may be a possible source of unscavengeable propanol. The protonated ether ion has to be in an excited state and within a few vibration times,  $\sim 10^{-12}$  sec, decomposition occurs. Thus, scavenging of this excited positive ion would not occur.

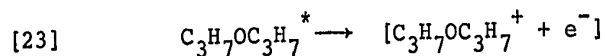
#### B. Kinetics

During irradiation of di-n-propyl ether with  $\gamma$ -rays or high energy electrons, excited molecules, positive ions and low energy ( $\sim 10^2$  eV) secondary electrons are generated. These ions and excited molecules are initially distributed in small elements of volume crudely approximated as spheres with diameters of the order of  $10^8$  Å and which are strung out along the paths of high energy electrons. This grouping of reactive species, which are close enough together and have a significant probability of reacting with each other, is called a spur. The excited molecules and ions might decompose or react to form free radicals so a spur can contain several types of reactive species. A spur can range in size from a large spur containing several radical pairs and ion pairs to a small spur with a single pair of radicals or ions. The spur under investigation in this work contains positive ion-electron pairs. This was verified by the sulfur hexafluoride and n-propylamine

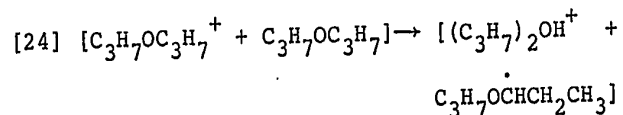


scavenging studies.

A high energy electron interacts with an ether molecule for about  $10^{-18}$  -  $10^{-16}$  sec exciting the molecule (24c). Ionization of the excited molecule

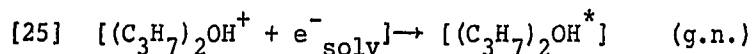


occurs in  $\sim 10^{-15}$  sec. Within such time a spur is formed. Entities in a spur will be represented by enclosing them in square brackets as in equation [23] and those following. The spur expands as the low energy electron moves away from the positive ion. The positive ion undergoes ion-molecule reaction and becomes a protonated ether ion



in about  $10^{-12}$  sec (37). The low energy electron travels through the liquid losing its excess energy by exciting or ionizing molecules of the liquid. The low energy electron usually travels less than  $100 \text{ \AA}$  (38) from the positive ion before being thermalized. The thermalized electron becomes localized in a cavity of the liquid. The localized electron transforms into the solvated state as dielectric relaxation occurs around the site of the localized electron. This takes place in about  $10^{-12}$  sec (39). The positive ion becomes solvated as well. The

coulombic attraction between the electron and the positive ion draws them back together. The ions undergo geminate neutralization in the spurs from  $\sim 10^{-11}$  -  $10^{-8}$  sec (40a).



Ions which escape geminate neutralization diffuse into the bulk medium and become free ions.

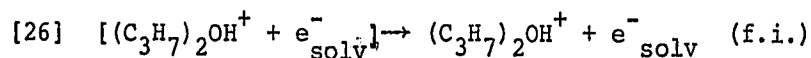
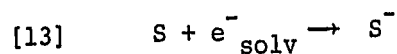


Figure 17 shows the calculated spectra of lifetimes of solvated electrons undergoing neutralization in three solvents. The spectrum for n-propyl ether would be similar to that for cyclohexane since their densities and dielectric constants are similar. A small fraction of the solvated electrons escape geminate neutralization in the spurs and become free ions. This fraction is 0.05 in propyl ether (37,41) and is the fraction of ions left at  $\sim 10^{-8}$  sec. Thus, the duration of the spur is placed at  $\sim 10^{-8}$  sec.

The free ions in the bulk medium continue to exist for a longer period of time. In a pure solvent, the positive ions and solvated electrons undergo random neutralization. In the propyl ether used, an impurity, presumably propionaldehyde in concentration  $< 10^{-4}$  M may be present. This would scavenge the solvated electrons and prevent the random neutralization of electrons with

positive ions. Evidence for the scavenging of free ion solvated electrons is presented in the homogeneous kinetics



section.

The reaction of solvated electrons in the bulk medium is described by homogeneous kinetics while that in the spurs requires the use of nonhomogeneous kinetics.

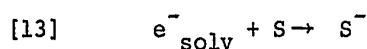
#### Part I. . . Homogeneous Kinetics of $e^-_{\text{solv}}$ (free ion) Reactions

Reactions which have been investigated by the pulse radiolysis technique occur in the bulk medium and are described by homogeneous kinetics. In the pulse radiolysis of propyl ether, the physical arrangement of the system was such that only the events with a duration of  $\sim 10^{-7}$  sec or longer could be followed. By such time, at room temperature, the electrons generated by a pulse have been solvated and the electrons that escaped neutralization reaction in the spurs have diffused into the bulk medium. The spur only exists for  $\sim 10^{-8}$  sec.

The rate constant for the first order decay of solvated electrons in propyl ether was calculated from the equation:

$$[iii] \quad k_1 = \frac{0.693}{t_{1/2}}$$

The rate constants  $k_1(e^-_{\text{solv}})$  are shown in Table X. At 0°C the observed first order decay is believed to be the reaction of electrons with an impurity, presumably propionaldehyde,

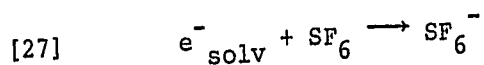


where S represents a scavenger. This is indicated by the observation made during pulse radiolysis experiment where  $t_{1/2}$  remained the same after the sample had received a considerable dose. Propionaldehyde is produced during radiolysis (1). If the decay of electrons had been other than reaction [13], the  $t_{1/2}$  would have decreased as the concentration of propionaldehyde product built up.

At -73°C and -124°C, the decay of solvated electrons proceeded from a higher order to first (noted as 2nd+1st, Table X). The first order tail of the decay is reaction [13] occurring in the bulk medium. The initial higher order could be a neutralization reaction in the tail end of the spur reactions. This suggests that at -73° and -124°C, the time duration of a spur has increased. In propyl ether, the dielectric constant  $\epsilon = 4.65$  (42) and viscosity  $\eta = 2.7$  cp at -73°C (calculated from  $E_\eta$  and data ref. 35) have increased from  $\epsilon = 3.4$  (41) and  $\eta = 0.398$  cp (35) at 25°C. The coulombic energy between the positive ion and solvated electron is lower at -73°C than at 20° due to higher dielectric constant. The mobilities of the ions

is less due to the increased viscosity. Thus the effect of decreasing the temperature would be to increase the neutralization times and the spectrum of the lifetimes of solvated electrons (Figure 17) in propyl ether would be shifted towards longer times. The spur would persist for  $\sim 10^{-7}$  sec at  $-73^\circ\text{C}$  and  $>10^{-7}$  sec at  $-124^\circ\text{C}$ . Events with a duration of  $10^{-7}$  sec could be observed by the pulse radiolysis system.

The rate constant for the reaction of solvated electrons with sulfur hexafluoride was calculated from the



equation derived from competition kinetics

$$[ii] \quad \frac{0.693}{t_{\frac{1}{2}}(\text{observed})} = \frac{0.693}{t_{\frac{1}{2}}(\text{ether})} + k_2[\text{SF}_6]$$

Rate constants  $k_2(\text{SF}_6 + e^-_{\text{solv}})$  at three temperatures are shown in Table X. Reaction [27] has an activation energy  $E_a = 3 \pm 1$  kcal/mole and is similar to the activation energy of viscosity  $E_\eta = 2.1$  kcal/mole.  $E_\eta$  was calculated from viscosity data in ref. (35). Extrapolation of the curve in Figure 16 to  $25^\circ\text{C}$  gives a rate constant  $k = 8 \times 10^{10} \text{ M}^{-1} \text{ sec}^{-1}$  which is in the region of a diffusion controlled rate.

The average lifetime at  $25^\circ\text{C}$  of solvated electrons

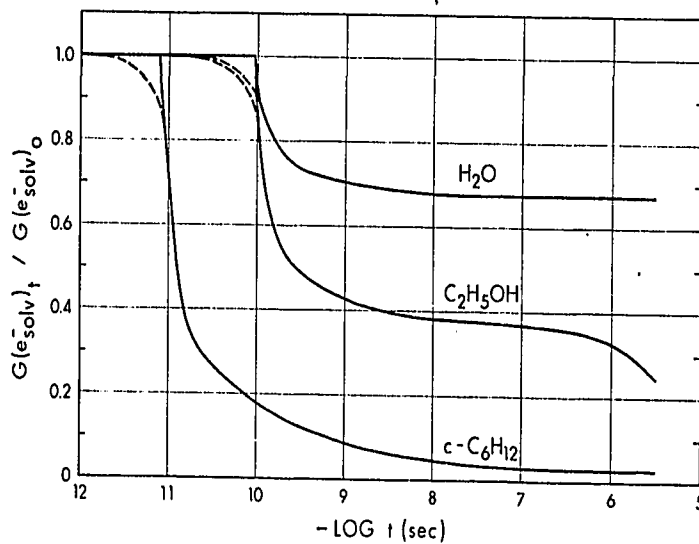


Figure 17. Calculated spectra of lifetimes of solvated electrons after instantaneous pulses of X rays in water, ethanol and cyclohexane at 20°C. Pulse dose  $<10^{16}$  eV/cm<sup>3</sup>. The dashed curves were arbitrarily drawn. The decline of the ethanol curve in  $\sim 10^{-6}$  sec is due to reaction [7]. Figure 17 was reproduced from ref. (40a).

in reaction [27] as calculated from the equation

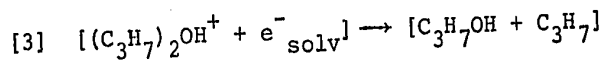
$$[\text{iv}] \quad t_a = \frac{1}{k_{25^\circ}[\text{SF}_6]}$$

is  $\sim 10^{-8}$  sec at  $[\text{SF}_6] = 10^{-3}$  M. The duration of a spur is  $\sim 10^{-8}$  sec. Thus, the scavenging curve of sulfur hexafluoride (Figure 6) represents scavenging of solvated electrons in the spurs.

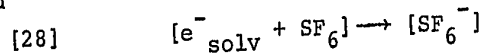
At  $-133^\circ\text{C}$ , a 2nd+1st order reaction was observed in sulfur hexafluoride solutions. The first order tail is due to the competition between reactions [13] and [27] in the bulk medium while the initial higher order reaction may be a spur neutralization reaction.

#### Part II Application of a Nonhomogeneous Kinetics Model

The description of a reaction that occurs in a spur requires the use of nonhomogeneous kinetics. It has been shown that the competing reactions



and



occur in spurs. The competition between reaction [3] and [28] was calculated using a statistical nonhomogeneous kinetics model described in the Appendix. In these calculations, the scavenging efficiency parameter  $\beta$  and  $(G_{e^-})_0'$

the total electron yield under consideration, were treated as adjustable parameters in order to obtain a calculated curve that best fit the experimental curve (see Figure 6). The best fit curve was obtained with  $\beta_- = 7 \times 10^{14} \text{ V/cm}^2$  and  $(G_{e^-})_0 = 1.9$ . The  $\beta$  parameter gives a measure of the ease of scavenging of electrons or positive ions in a given scavenging system. In comparing the scavenging curves of sulfur hexafluoride and n-propylamine (Figures 6 and 8), it is seen that the electrons are two orders of magnitude more readily scavengable than the protonated ether ions. Assuming that both scavengers have the same encounter efficiencies,  $\beta_+ = 7 \times 10^{12} \text{ V/cm}^2$  is obtained for the scavenging of protonated ether ion by n-propylamine. Since  $\beta$  depends on the sum of  $\frac{bD}{\lambda^2}$  of the positive ion or electron and its scavenger, the two orders of magnitude difference between  $\beta_+$  and  $\beta_-$  means that (see Appendix)

$$\left[ \frac{b_{D-}}{\lambda_-^2} + \frac{b_{SF_6}^{D_{SF_6}}}{\lambda_{SF_6}^2} \right] = 100 \left[ \frac{b_{D+}}{\lambda_+^2} + \frac{b_{amine}^{D_{amine}}}{\lambda_{amine}^2} \right]$$

Since the positive ion is probably a little bigger than the amine molecule,  $\frac{b_{D+}}{\lambda_+^2}$  is probably just a little smaller than  $\frac{b_{amine}^{D_{amine}}}{\lambda_{amine}^2}$ . Assuming  $\frac{b_{D-}}{\lambda_-^2} \gg \frac{b_{SF_6}^{D_{SF_6}}}{\lambda_{SF_6}^2}$ , it appears that

$$\frac{b_{D-}}{\lambda_-^2} \approx 200 \frac{b_{D+}}{\lambda_+^2}$$



Since  $\frac{b_-}{\lambda_-^2}$  and  $\frac{b_+}{\lambda_+^2}$  would be of the same order of magnitude and the diffusion coefficients are proportional to the mobilities, the mobility of the solvated electrons is about two orders of magnitude greater than that of the positive ions in propyl ether.

Greater electron mobilities than that of positive ions have been observed and measured in hydrocarbons (43-45). Propyl ether is similar to a hydrocarbon with respect to dielectric constant and viscosity. In methylcyclopentane (43), the electron mobility was observed to be about an order of magnitude greater than that of the positive ion. In some hydrocarbons, as shown in Table XI the measured electron mobilities are about two-three orders of magnitude greater than positive ion mobilities.

### C. Solvated Electron Optical Absorption Spectrum

A transient optical absorption in the IR region was observed during pulse radiolysis of propyl ether. The absorption was assigned to solvated electrons, as the addition of electron scavenger, sulfur hexafluoride, decreased the half-life of the absorbing species.

Solvated electrons in propyl ether absorb light in the IR region with a maximum lying above 1600 nm (Figure 13). In diethyl ether, the absorption maximum ( $\lambda_{\max}$ ) was observed at 2100 nm at 25°C (19). The trend in the position

TABLE XIElectron and Positive Ion Mobilities at ~23°C

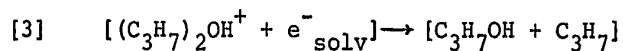
Compound	(44) $\mu^-$ ( $\text{cm}^2\text{V}^{-1}\text{sec}^{-1}$ )	(45) $\mu^+$ ( $\text{cm}^2\text{V}^{-1}\text{sec}^{-1}$ )	(46) $\epsilon$	(47) $\eta$ (centipoise)
n-Pentane	0.16	$0.82 \times 10^{-3}$	1.84	0.23
n-Hexane	0.09	$0.64 \times 10^{-3}$	1.89	0.31
Cyclohexane	0.35	$0.21 \times 10^{-3}$	2.02	0.97

of  $\lambda_{\text{max}}$  suggests that it is a function of the class of compound as well as of the dielectric properties of the liquid (19). For polar compounds such as alcohols and water, the  $\lambda_{\text{max}}$  are in the region from 580-820 nm; the amines and ammonia from 1350-1900 nm; and for weakly polar ethers, ~2100 nm.

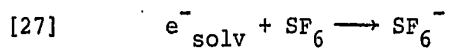
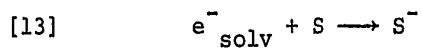
Decreasing the temperature was observed to shift the absorption spectrum of propyl ether towards lower wavelengths. This temperature shift has also been observed in water (25) and in alcohols (48). Lowering the temperature narrows the spectrum slightly and shifts the energy at the absorption maximum towards higher energies. The displacement towards higher energies has been ascribed to thermal shrinkage of the cavity (29).

V C O N C L U S I O N

Based on scavenging studies, the mechanism proposed for the formation of propanol in the  $\gamma$ -radiolysis of liquid n-propyl ether is



The participation of solvated electrons in reactions during radiolysis of n-propyl ether was confirmed by its absorption spectrum. Absorption spectra of solvated electrons in the bulk medium were obtained at three temperatures. Reactions [13] and [27] were found to have similar activation energy  $E_a = 3$  kcal/mole.



REFERENCES

1. A. S. Newton, *J. Phys. Chem.*, 61, 1485 (1957).
2. M. K. M. Ng and G. R. Freeman, *J. Amer. Chem. Soc.*, 87, 1635 (1965).
3. P. Gray and A. Williams, *Chem. Rev.*, 59, 239 (1959).
4. E. J. Hart, S. Gordon and J. K. Thomas, *J. Phys. Chem.*, 68, 1271 (1964).
5. G. R. Freeman, *Actions Chimiques et Biologiques des Radiations*, 14, 73 (1970).
6. Ibid, p.131.
7. G. Czapski and H. A. Schwarz, *J. Phys. Chem.*, 66, 471 (1962).
8. E. J. Hart and J. W. Boag, *J. Amer. Chem. Soc.*, 84, 4090 (1962).
9. J. W. Boag and E. J. Hart, *Nature*, 197, 45 (1963).
10. M. S. Matheson, W. A. Mulac and J. Rabani, *J. Phys. Chem.*, 67, 2613 (1963).
11. D. C. Walker, *Can. J. Chem.*, 44, 2226 (1966).
12. H. A. Schwarz, *J. Amer. Chem. Soc.*, 77, 4960 (1955).
13. E. Collinson, F. S. Dainton, D. R. Smith and S. Tazuki, *Proc. Chem. Soc.*, 140 (1962).
14. G. V. Burton, F. S. Dainton and M. Hammerli, *Trans. Faraday Soc.*, 63, 1191 (1967).
15. S. Gordon, E. J. Hart, M. S. Matheson, J. Rabani and J. K. Thomas, *J. Amer. Chem. Soc.*, 85, 1375 (1963).

16. Solvated Electron, Advances in Chemistry Series, 50, American Chemical Society Publications (1965).
17. M. C. Sauer Jr., S. Arai and L. M. Dorfman, J. Chem. Phys., 42, 708 (1965).
18. J. L. Dye, M. G. Debacker and L. M. Dorfman, J. Chem. Phys., 52, 6251 (1970).
19. L. M. Dorfman, F. Y. Jou and R. Wageman, Berichte der Bunsen-Gesellschaft, 75, 681 (1971).
20. J. H. Baxendale and M. A. J. Rogers, J. Phys. Chem., 72, 3849 (1968).
21. J. H. Baxendale, D. Beaumont and M. A. J. Rodgers, Trans. Faraday Soc., 66, 1997 (1970).
22. E. J. Hart and M. Anbar, "The Hydrated Electron", Wiley Interscience, New York, 1970. (a) p.126; (b) p.127; (c) p.131; (d) p.146.
23. M. Anbar and E. J. Hart, J. Phys. Chem., 69, 271 (1965).
24. G. R. Freeman, Radiation Chemistry, 1966. (a) p.108; (b) p.142; (c) p.143.
25. W. C. Gottschall and E. J. Hart, J. Phys. Chem., 71, 2102 (1967).
26. S. Arai and M. C. Sauer, Jr., J. Chem. Phys., 44, 2297 (1966).
27. M. G. Robinson, K. N. Jha and G. R. Freeman, J. Chem. Phys., 55, 4933 (1971).
28. R. R. Hentz, Farhataziz and E. M. Hansen, J. Chem. Phys., 55, 4974 (1971).

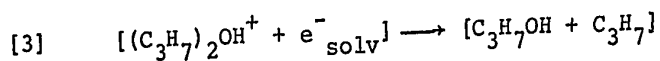
29. U. Schindewolf, *Angew. Chem. Internat. Edit.*, 7, 196 (1968).
30. J. Jortner, S. A. Rice and E. G. Wilson, "Metal Ammonia Solutions", eds. G. Lepoutre and M. J. Sienko, Benjamin, Inc., New York, 1964 p.222.
31. J. Jortner, *Actions Chimiques et Biologiques des Radiations*, 14, 62 (1970).
32. M. Gold and W. L. Jolly, *Inorg. Chem.*, 1, 818 (1962).
33. E. M. Fielden and E. J. Hart, *Trans. Faraday Soc.*, 63, 2975 (1967).
34. A. O. Allen, "The Radiation Chemistry of Water and Aqueous Solutions", D. Van Nostrand Co. Inc., New York, 1961 p.21.
35. J. Timmermans, *Physico-Chemical Constants of Pure Organic Compounds*, Elsevier, Amsterdam, 1950, Vol. 1.
36. P. Gray, R. Shaw and J. C. J. Thynne, *Progress in Reaction Kinetics*, 4, 104 (1967).
37. K. Bansal and S. J. Rzed, *J. Phys. Chem.*, 74, 2888 (1970).
38. G. R. Freeman, *Rad. Res. Rev.*, 1, 36 (1968).
39. Calculated from data in "Tables of Dielectric Dispersion Data for Pure Liquids and Dilute Solutions", NBS Circular 589, (1958).
40. G. R. Freeman, *Estratto da Quaderni de la Ricerca Scientifica*, 67 (1970).  
(a) p.41; (b) p.51.

41. G. R. Freeman and J. M. Fayadh, *J. Chem. Phys.*, 43, 86 (1965).
42. P. Tremaine, Chemistry Department, University of Alberta, private communications.
43. D. Stover and G. R. Freeman, *J. Chem. Phys.*, 48, 3902 (1968).
44. W. F. Schmidt and A. O. Allen, *J. Chem. Phys.*, 52, 4788 (1970).
45. P. H. Tewari and G. R. Freeman, *J. Chem. Phys.*, 49, 954 (1968).
46. Landolt and Bornstein, *Zahlenwerte und Funktionen*, Bd II, Tl. 6.
47. R. W. Gallant, *Physical Properties of Hydrocarbons*, Gulf, Houston, Texas, 1968, Vol. 1.
48. G. Bolton, K. N. Jha and G. R. Freeman, to be published.

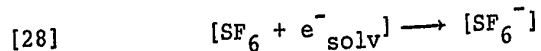


A P P E N D I XA Nonhomogeneous Kinetics Model (40b)

Propanol is formed by the spur reaction



In the presence of sulfur hexafluoride, the reaction



competes with reaction [3]. The competition between [3] and [28] is described in a nonhomogeneous kinetic model of charge scavenging. If one assumes that each electron yields a molecule of propanol, the decrease in propanol yield caused by sulfur hexafluoride scavenging of solvated electrons during the radiolysis of propyl ether can be calculated using the equation:

$$\Delta G_{(propanol)} = \frac{\sum N(y) \phi_- (1 - e^{-r/y})}{\sum N(y)} \cdot (G_{e^-})_0$$

where

$N(y)$  is the relative number of positive ion-thermalized electron pairs that have an initial separation distance  $y$ .

$\phi_-$  is the probability that scavenging reaction [28] occurs before reaction [3]

$(1 - e^{-r/y})$  is the fraction of electrons that remain in the spur

$(G_{e^-})_0$  is the total yield of electrons being considered and which are found in the spurs and in the bulk medium.

In the propyl ether used, the free ion yield of electrons is scavenged by an impurity and does not contribute to the propanol yield. The fraction of electrons that become free ions is given by the Boltzman factor

$$\text{Fraction (fi)} = e^{-r/y}$$

where  $r$  is the distance between positive ion and electron at which the coulombic energy of attraction equals  $kT$ .

The value of  $r$  is given by the equation

$$r = \xi^2 / \epsilon kT$$

where

$\xi$  is the charge on an electron

$\epsilon$  is the static dielectric constant of propyl ether

$k$  is Boltzman's constant

$T$  is the Absolute temperature

The value of  $\phi_-$ , the probability that electrons are scavenged in the spurs is calculated from the equation

$$\phi_- = 1 - (1 - f_- N_s)^{\beta_- \nu}$$

where  $(1 - f_- N_s)^{\beta_- \nu}$  is the probability that electrons will not be scavenged and

$f_-$  is the encounter efficiency of the scavenging reaction (assumed to be unity in this work).

$N_s$  is the mole fraction of sulfur hexafluoride.

The parameter  $\beta_-$  is given by the following equation:

$$\beta_- = \frac{\left[ \frac{b_- D_-}{\lambda_-^2} + \frac{b_s D_s}{\lambda_s^2} \right]}{(u_- + u_+)}$$

where

$D_-$  and  $D_s$  are diffusion coefficients of electron and sulfur hexafluoride molecule

$b_-$  and  $b_s$  are the number of new molecules each encounters per diffusion jump

$\lambda_-$  and  $\lambda_s$  are the average jump distances

$u_-$  and  $u_+$  are the mobilities of the electron and positive ion

The parameter  $\nu$  is given as

$$\nu = \frac{6\epsilon(y^3 - r_o^3)}{4.32 \times 10^{-7} d}$$

where

$r_o$  is the center-to-center distance of the positive ion and electron at the instant the final electron jump occurs in the absence of sulfur hexafluoride

$d$  is a constant taken as unity.

In determining the value of  $v$ ,  $y^3$  is considered to be much greater than  $r_o^3$  so that  $r_o$  may be neglected.

In calculating the decrease of propanol yield at a given mole fraction of sulfur hexafluoride, the  $\beta$  parameter is treated as an adjustable parameter along with  $(G_e)_o$  in order to obtain a calculated decrease that best fits the experimental decrease. The values of the parameters used are:

$$\beta = 7 \times 10^{14} \text{ V/cm}^2$$
$$(G_{e^-})_o = 1.9$$

The fraction of free ions,  $e^{-r/y}$ , is 0.05.